Effects of temperature and circulation on the population dynamics of *Calanus finmarchicus* in the Gulf of St. Lawrence and Scotian Shelf: Study with a coupled, three-dimensional hydrodynamic, stage-based life history model

Bruno A. Zakardjian,[1] Jinyu Sheng,[2] Jeffrey A. Runge,[3] Ian McLaren,[4] Stéphane Plourde,[5,6] Keith R. Thompson,[2] and Yves Gratton[7]

Received 27 March 2002; revised 23 January 2003; accepted 28 May 2003; published 4 November 2003.

[1] We developed a physical-biological model for the Gulf of St. Lawrence (GSL) and Scotian Shelf (SS) by coupling a stage-based life-history model of the planktonic copepod *Calanus finmarchicus* to a three-dimensional ocean circulation model. The life-history model consists of 13 morphologically distinct life stages of *C. finmarchicus*, with stage-specific and temperature-dependent molting rates. The model also includes stage-specific vertical distribution and seasonally varying diapause, egg production, and stage-specific mortality rates. The model domain covers the eastern Canadian shelf from 55°W to 72°W and from 39°N to 52°N, including the Gulf of St. Lawrence, Scotian Shelf, and Gulf of Maine. A comparison of a 1-year simulation with observations indicates that the physical-biological model reasonably describes the observed abundance and distribution of *C. finmarchicus* in this region. To determine the effects of ocean circulation in the *C. finmarchicus* population dynamics, we divided the GSL-SS region into eight sub-areas and compared the net fluxes of *C. finmarchicus* across lateral boundaries to the net production in each sub-area. We found that the annual cross-boundary exchange rates constitute from <1% to 39% of the local net production, indicating that the horizontal transport of *C. finmarchicus* by the ocean currents can play a very important role in the dynamics of local *C. finmarchicus* populations. The results provide insights into the mechanisms of exchange in the GSL-SS system, as put forward in recent hypotheses. *INDEX TERMS:* 4855 Oceanography: Biological and Chemical: Plankton; 4532 Oceanography: Physical: General circulation; 4255 Oceanography: General: Numerical modeling; *KEYWORDS: Calanus finmarchicus*, GLOBEC, hydrodynamic model, life-cycle model, Gulf of St. Lawrence, Scotian Shelf

Citation: Zakardjian, B. A., J. Sheng, J. A. Runge, I. McLaren, S. Plourde, K. R. Thompson, and Y. Gratton, Effects of temperature and circulation on the population dynamics of *Calanus finmarchicus* in the Gulf of St. Lawrence and Scotian Shelf: Study with a coupled, three-dimensional hydrodynamic, stage-based life history model, *J. Geophys. Res.*, *108*(C11), 8016, doi:10.1029/2002JC001410, 2003.

1. Introduction

[2] *Calanus finmarchicus* is a dominant zooplankton species in the North Atlantic Ocean [e.g., *Marshall and Orr*, 1955; *Colebrook*, 1982; *Planque et al.*, 1997; *Planque and Batten*, 2000] and its adjacent seas including the Gulf of St. Lawrence and Scotian Shelf [*Tremblay and Roff*, 1983; *Runge and Simard*, 1990; *de Lafontaine et al.*, 1991]. It is an important prey for early life stages of several commercially important fish stocks, mainly cod and redfish, both in the eastern [e.g., *Hansen et al.*, 1994; *Fossum and Ellertsen*, 1994] and western North Atlantic [*Anderson*, 1994; *Albikovskaya and Gerasimova*, 1993; *Sameoto et al.*, 1994; *Runge and de Lafontaine*, 1996]. The population dynamics of *C. finmarchicus* are greatly affected by ocean currents that may transport it from the deep North Atlantic, where it over-winters at depth, to the relatively shallow shelf regions [e.g., *Backhaus et al.*, 1994; *Aksnes and Blindheim*, 1996; *Slagstad and Tande*, 1996; *Bryant et al.*, 1998; *Gaard*, 1999,

[1]Institut des Sciences de la Mer de Rimouski (ISMER), Université du Québec à Rimouski, Rimouski, Quebec, Canada.
[2]Department of Oceanography, Dalhousie University, Halifax, Nova Scotia, Canada.
[3]Ocean Process Analysis Laboratory, University of New Hampshire, Durham, New Hampshire, USA.
[4]Department of Biology, Dalhousie University, Halifax, Nova Scotia, Canada.
[5]Département de Biologie, Université Laval, Sainte-Foy, Quebec, Canada.
[6]Now at Fisheries and Ocean Canada, Maurice Lamontagne Institute, Mont-Joli, Quebec, Canada.
[7]INRS-Eau, Sainte-Foy, Quebec, Canada.

0148-0227/03/2002JC001410

2000; *Pedersen et al.*, 2001]. Copepod production may act as a link between hydrodynamic effects of climatic variability and fisheries productivity [*Cushing*, 1984; *Runge*, 1988; *Anderson*, 1994; *Hansen et al.*, 1994; *Skreslet*, 1997; *Runge et al.*, 1999; *Sundby*, 2001]. Because of this potential for physical-biological linkage, *C. finmarchicus* was identified as one of the key species in Global Ocean Ecosystems Dynamics (GLOBEC) research programs for the North Atlantic, including U.S. GLOBEC [e.g., *Wiebe et al.*, 1996], the Trans-Atlantic Study of *Calanus* [*Tande and Miller*, 2000], and GLOBEC-Canada [*Mackas and deYoung*, 2001], all with a major focus on interactions between circulation and *C. finmarchicus* population dynamics.

[3] The Atlantic component of GLOBEC-Canada examined the role of circulation and temperature on the distribution and abundance of *C. finmarchicus* in eastern Canadian waters, in particular the Gulf of St. Lawrence (hereinafter GSL) and Scotian Shelf (SS). Variations in circulation and other environmental features, such as temperature and surface winds, influence the distribution and abundance of zooplankton, notably *C. finmarchicus* [*Runge*, 1988; *Herman et al.*, 1991; *Sameoto et al.* 1994; *Runge and Simard*, 1990; *Head et al.*, 1999]. Geographically, the GSL-SS can be considered as an extended estuarine shelf system under the influence of the freshwater discharge from the St. Lawrence River watershed. The inshore and offshore branches of the Labrador Current and the north-bound of the Gulf Stream also play an important role in controlling its circulation. *Plourde and Runge* [1993] hypothesized that the Lower Estuary acts as a zooplankton "pump," supplying young individuals to the summer population of *Calanus* in the Gulf of St. Lawrence. Transport from the Gulf of St. Lawrence, in turn, was thought to be the dominant source of zooplankton to the Scotian Shelf [*Herman et al.*, 1991], although more recent observations implicate an important role of immigration from the slope water offshore [*Head et al.*, 1999].

[4] As part of the GLOBEC-Canada program, we developed a physical-biological model for the GSL-SS (Figure 1) system by linking a three-dimensional (3D) ocean circulation model (CANDIE [*Sheng*, 2001; *Sheng et al.*, 1998, 2001; J. Sheng et al., Seasonal mean circulation over the eastern Canadian shelf, with emphasis on the Gulf of St. Lawrence and Scotian Shelf, manuscript in revision for *Journal of Geophysical Research*, 2003 (hereinafter referred to as Sheng et al., manuscript in revision, 2003]) that predicts regional temperature, salinity, and flow to a seasonal life-history model of *C. finmarchicus*. Our main objective is to determine how *C. finmarchicus* maintains itself in the extended shelf system given the strong, seasonal variations in the large-scale hydrography and circulation. To what extent does the estuarine advective flow distribute *C. finmarchicus* among regions of the shelf system? What are the major sources and sinks for the population within this advective regime? The model and the results we describe here are directed toward answering these questions through a "climatological run" covering an annual cycle with both realistic regional circulation and *C. finmarchicus* abundance and stage-structure for the GSL-SS region. We present the physical-biological model in section 2. The model results are described in section 3. In this section, we compare the model results to observed

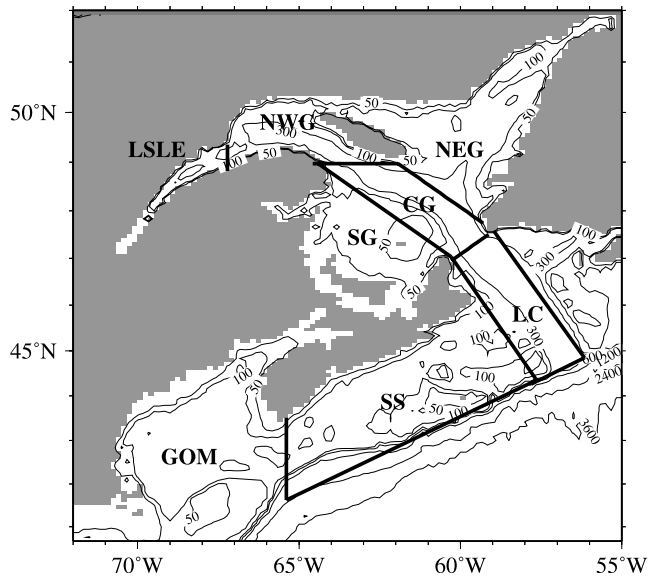

Figure 1. Locations and bathymetry of the sub-areas discussed in the text: Lower St. Lawrence Estuary (LSLE), northwest Gulf of St. Lawrence (NWG), northeast Gulf (NEG), southern Gulf (SG), central Gulf (CG), Laurentian Channel (LC), Scotian Shelf (SS), and Gulf of Maine (GOM). Boundaries indicate sites of flux calculations.

life history cycles and seasonal abundance patterns in the GSL-SS and we estimate the effects of circulation on the dynamics of local *C. finmarchicus* populations. We discuss the implications and future directions leading from these results in section 4.

2. Model Formulation

[5] Given the main objective or our study, which is to quantify advection-induced mixing of sub-populations in a large-scale system, we use a stage-based model embedded in an Eulerian framework. In an Eulerian approach, the biological rates (development, mortality, reproduction) depend on the local environmental conditions but neglect individual histories. While this approach is less efficient in describing individual growth than individual-based models used in other studies of copepod population dynamics [e.g., *Tande and Slagstad*, 1992; *Miller and Tande*, 1993; *Carlotti and Radach*, 1996; *Miller et al.*, 1998], it does allow easier quantitative description of exchange between sub-populations at regional scale. The stage-based model we developed follows the pioneering work of *Wroblewski* [1982] in a form similar to the model described by *Lynch et al.* [1998] for the life history of *C. finmarchicus* in the Gulf of Maine (GOM). The life-history model comprises the egg, six naupliar (NI to NVI), and six copepodid (CI to CVI) stages of the *C. finmarchicus* life cycle [*Marshall and Orr*, 1955]. Adults (stage CVI) are further divided into males (CVIm) and reproductively immature (CVIfj) and mature females (CVIfm). In addition, the model accounts for mortality and development during the diapausing CV (CVd) stage. The time-varying abundance at each stage (number per cubic meter) is determined by the combined effects of (1) advection, (2) turbulent mixing, (3) stage-specific

vertical distribution and swimming behavior (except eggs), (4) stage-specific and temperature-dependent molting rates, (5) stage-specific, seasonally varying, and temperature-dependent mortality rates, and (6) for eggs, seasonally varying spawning by CVI females. Description of the CANDIE results that set environmental conditions, *C. finmarchicus* life history model and coupling with the CANDIE fields are detailed in the subsequent sections.

2.1. Environmental Conditions: The CANDIE 3D Hydrodynamic Model

[6] The hydrodynamic model used in this study is the 3D nonlinear z-level ocean circulation model known as CANDIE [*Sheng et al.*, 1998]. This model has been subjected to rigorous testing (D. Wright, personal communication, 2002) and successfully applied to various modeling problems on the shelf, which include wind-driven circulation over an idealized coastal canyon [*Sheng et al.*, 1998], nonlinear dynamics of the Gaspé Current [*Sheng*, 2001], tidal circulation in the GSL [*Lu et al.*, 2001], seasonal circulation over the northwest Atlantic Ocean [*Sheng et al.*, 2001], and most recently, seasonal circulation in the western Caribbean Sea [*Sheng and Tang*, 2003]. In the present study, CANDIE was applied to the eastern Canadian shelf between 55°W and 72°W and between 41°N and 52°N (Figure 1). The model horizontal resolution is about 13 km in longitude and 9 km in latitude. There are 21 unevenly spaced z-levels in the vertical, with higher resolution near the surface.

[7] CANDIE was run in diagnostic mode with the model temperature and salinity at each time step interpolated linearly from the two nearest values for the seasonal-mean climatology (Sheng et al., manuscript in revision, 2003). Wind stress was set to zero in the momentum equation, but 12-hourly wind fields with a resolution of 2.5° obtained from the European Centre for Medium-Range Weather Forecasts were used to estimate the surface mixing depth and the vertical mixing coefficients. A time-varying eastward flow was introduced at the head of St. Lawrence Estuary to represent freshwater runoff from the St. Lawrence River. At the model lateral closed boundaries the normal flow and tangential stress of the currents were set to zero (free-slip conditions). Along the model open boundaries, an explicit Orlanski radiation condition [*Orlanski*, 1976] was first used to determine whether the open boundary is passive (outward propagation) or active (inward propagation). If the open boundary is passive, the normal flow at the open boundary is radiated outward to allow any perturbation generated inside the model domain to propagate outward as freely as possible. If the open boundary is active, the normal flow at the open boundary is restored to the seasonal mean climatology at each z-level with the timescale of 15 days. In addition, three steady barotropic jets were specified at the eastern open boundary to simulate the influence of the Labrador Current: one through the Strait of Belle Isle, and the other two near St. Pierre Bank to the south of Newfoundland.

[8] Figure 2 shows the temperature fields at the model's top z-level (centered at 5 m from surface) interpolated from the seasonal mean climatology constructed for the region by Sheng et al. (manuscript in revision, 2003). The near-surface waters in the GSL-SS region are relatively cold and spatially uniform in winter (January to March), and warm up gradually from south to north in spring (April to June). With continuous surface heating, the near-surface temperature in the region reaches its maximum in summer (July to September) and then decreases gradually in fall (October to December). The time-depth distributions of water temperatures in the upper 300 m averaged horizontally over sub-regions (Figure 3) exhibit a gradual establishment of the upper-ocean stratification in spring and summer, and relatively rapid establishment of cold and weakly stratified waters in fall and winter. This is consistent with the fact that the upper ocean in this region has relatively weak vertical mixing in spring and summer from the stable stratification associated with surface heating, but strong convective mixing in fall and winter associated with surface cooling (Sheng et al., manuscript in revision, 2003). The interpolated temperature and salinity fields are characterized as the time evolution from a two-layer system in winter (a cold, relatively fresh surface layer overlying a warmer and saltier bottom layer) to a three-layer system in summer (a warm, relatively fresh surface layer, a cold intermediate layer, and a warmer and saltier bottom layer) in the LSLE and GSL, as described by *Koutitonsky and Bugden* [1991]. The maximum and minimum interpolated temperatures at each z-level also agree reasonably well with the previous estimates in the region [e.g., *Koutitonsky and Bugden*, 1991; *Petrie et al.* 1996]. The model calculated 3D currents reproduce many well-known large-scale circulation features in the region (Figure 4), including a year-round cyclonic gyre over the northwestern GSL, southeastward outflow through the western Cabot Strait, and southwestward flow on the SS with relatively strong coastal and shelf-break jets.

2.2. *C. finmarchicus* Life-History Model

[9] The generic formulation for the abundance of stages NII to CV can be written as equations (1)–(5) in Table 1, where $\vec{U}$ is the 3D velocity vector from the CANDIE model, K_z represents vertical mixing, and the terms in the second set of brackets on the right-hand side represent the biological processes (development, mortality, swimming, etc.). The terms μ_{Ni} and μ_{Ci} represent stage-specific molting rates, m_{Ni} and m_{Ci} are mortality rates, and W_{Ni} or W_{Ci} are vertical swimming speeds of the life stages (here the subscripts N and C represent naupliar and copepodid stages, respectively).

[10] Stage-specific molting rates act as cascading transfer functions from eggs to diapausing CV, adult males and immature females. The molting rates were defined in terms of stage-specific, temperature-dependent development times (Table 2) estimated from laboratory experiments [*Campbell et al.*, 2001b], which differ only slightly from estimates by *McLaren et al.* [1988]. We assume that development time, to stage i(either naupliar or copepodid), has a corresponding stage-specific molting rate $\mu_i = \ln(2)/(D_i - D_{i-1})$. The term $\ln(2)$ in the numerator follows from $(1/C_i)\, dC_i/dt = \mu_i$ and the experimental convention that $\frac{1}{2}$ of the population of stage $i-1$ molts to stage i after the time $(D_i - D_{i-1})$. We tested the ability of this formulation to simulate cohort development in a simple preliminary simulation assuming constant temperature, an initial egg population, no mortality, and sterile adults. Figure 5 shows that the model preserves the initial stock as the cohort matures. Development time to adult is somewhat longer (10–20 days) than predicted by the theoretical

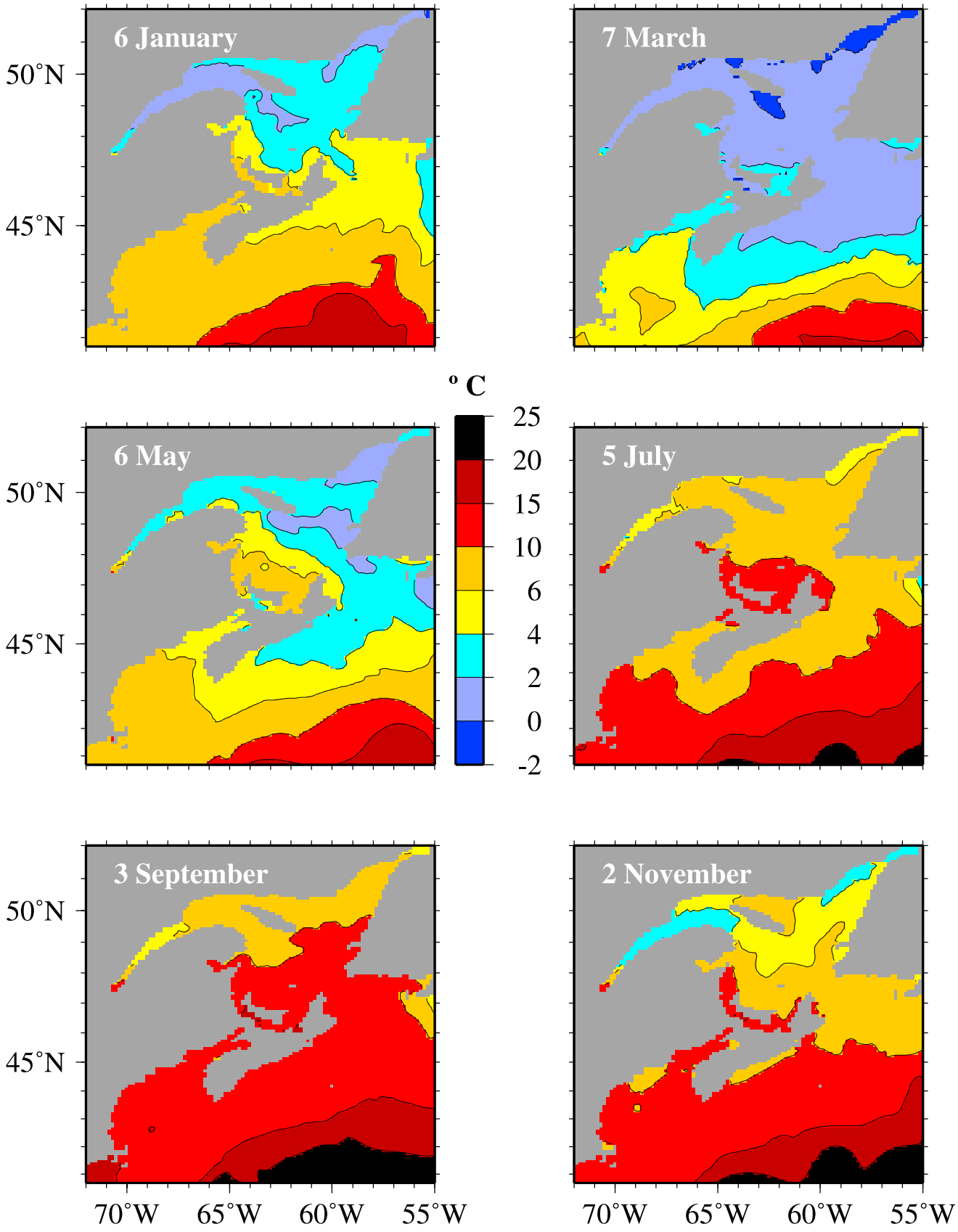

Figure 2. Simulated seasonal patterns of the sea-surface temperature produced by the CANDIE physical model.

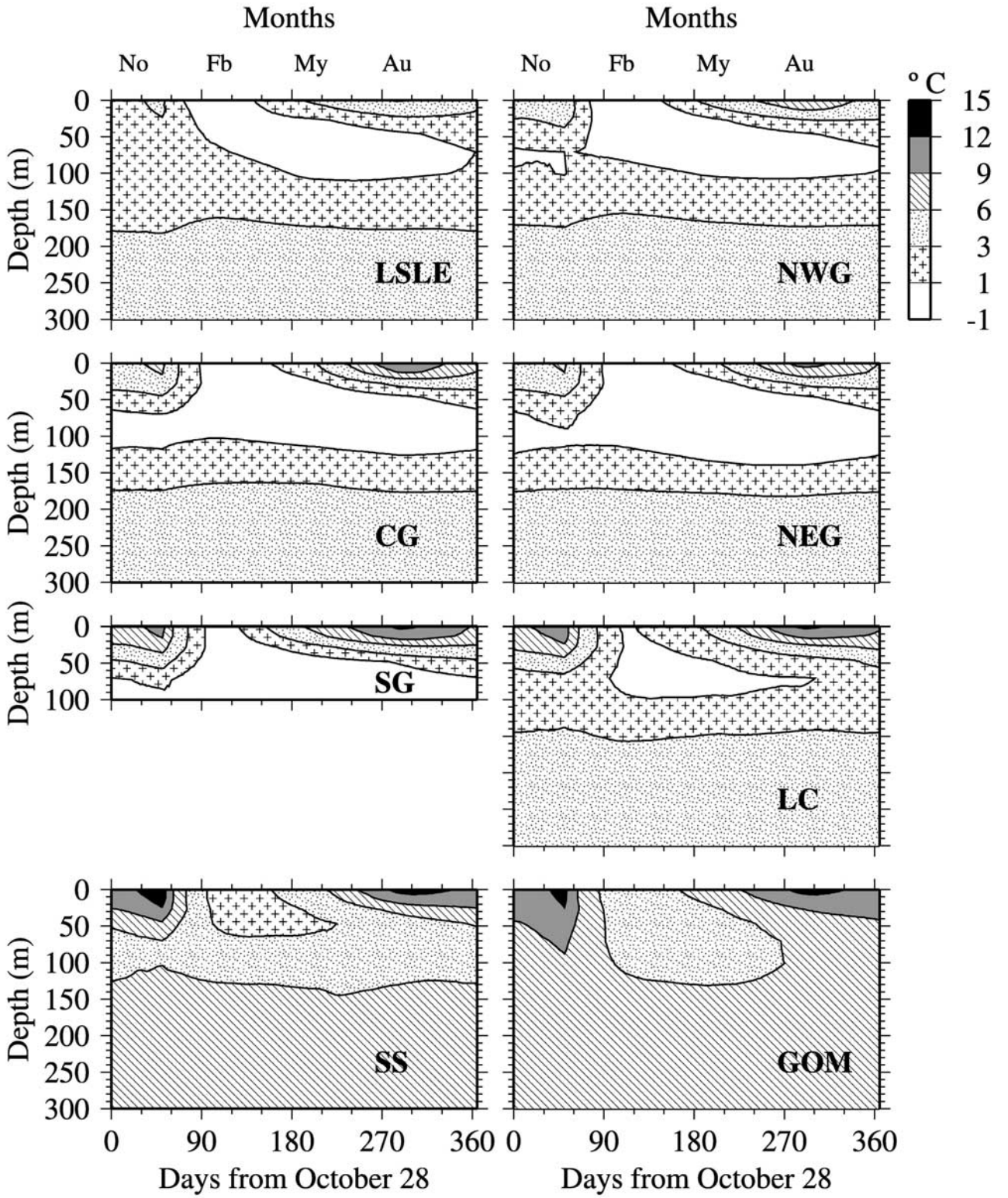

Figure 3. Seasonal trends, as simulated by CANDIE, of the vertical distribution of temperature in the upper 300 m. Regional abbreviations as in Figure 1.

Belehradek function; on the other hand, premature maturation, which is inherent in the Eulerian approach, is less than 20% in all cases.

[11] The governing equations for the abundance of eggs, adults, and CV in diapause are different from the generic equations (1)–(5), in order to include specific biological processes for these stages. First, at the end of their intermolt period, CVs were allocated either to enter diapause or to molt to adult in percentages determined by a seasonally varying function, Diap (equation (11)) where t is time and LagT

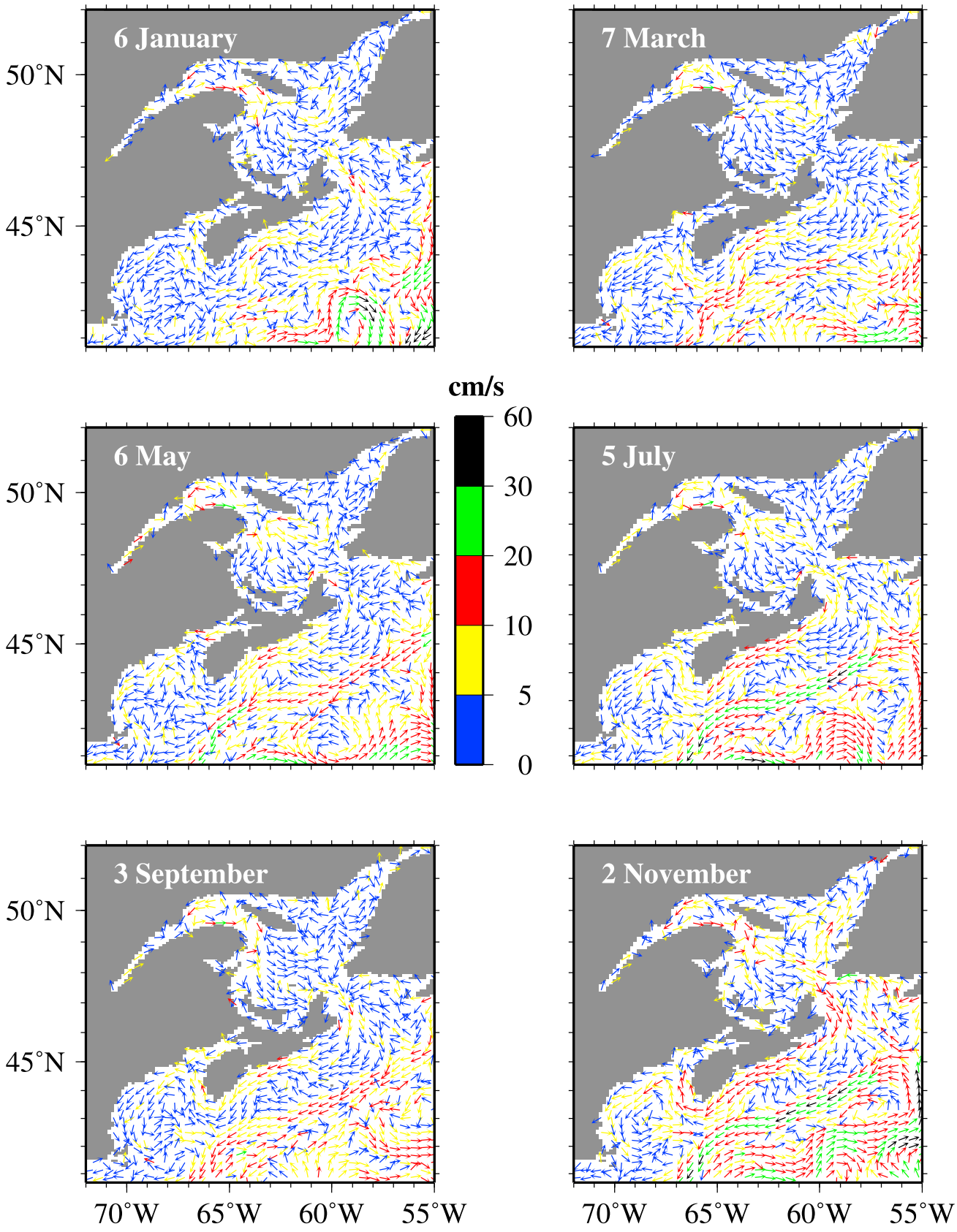

Figure 4. Simulated seasonal patterns of the surface circulation calculated by the CANDIE model. Colors represent current speed.

Table 1. System of Differential Equations and Biological and Climatological Functions Used for the Spatial and Temporal Evolution of the State Variables[a]

Equation	Number
$\frac{\partial}{\partial t}(\mathrm{Eggs}) + \nabla\left[\vec{U}.\mathrm{Eggs}\right] = \frac{\partial}{\partial z}\left[K_z \frac{\partial}{\partial z}(\mathrm{Eggs})\right] + \left[-\mu_{\mathrm{Eggs}}.\mathrm{Eggs} + \mathrm{Spawn}.\mathrm{CVIfm} - m_{\mathrm{Eggs}}.\mathrm{Eggs}\right]$	(1)
$\frac{\partial}{\partial t}(\mathrm{NI}) + \nabla\left[\vec{U}.\mathrm{NI}\right] = \frac{\partial}{\partial z}\left[K_z \frac{\partial}{\partial z}(\mathrm{NI})\right] + \left[-\mu_{\mathrm{NI}}.\mathrm{NI} + \mu_{\mathrm{Eggs}}.\mathrm{Eggs} - m_{\mathrm{NI}}.\mathrm{NI} + \frac{\partial}{\partial z}(W_{\mathrm{NI}}\mathrm{NI})\right]$	(2)
$\frac{\partial}{\partial t}(\mathrm{NII}) + \nabla\left[\vec{U}.\mathrm{NII}\right] = \frac{\partial}{\partial z}\left[K_z \frac{\partial}{\partial z}(\mathrm{NII})\right] + \left[-\mu_{\mathrm{NII}}.\mathrm{NII} + \mu_{\mathrm{NI}}.\mathrm{NI} - m_{\mathrm{NII}}.\mathrm{NII} + \frac{\partial}{\partial z}(W_{\mathrm{NII}}\mathrm{NII})\right]$	(3)
$\frac{\partial}{\partial t}(\mathrm{CI}) + \nabla\left[\vec{U}.\mathrm{CI}\right] = \frac{\partial}{\partial z}\left[K_z \frac{\partial}{\partial z}(\mathrm{CI})\right] + \left[-\mu_{\mathrm{CI}}.\mathrm{CI} + \mu_{\mathrm{NVI}}.\mathrm{NVI} - m_{\mathrm{CI}}.\mathrm{CI} + \frac{\partial}{\partial z}(W_{\mathrm{CI}}\mathrm{CI})\right]$	(4)
$\frac{\partial}{\partial t}(\mathrm{CII}) + \nabla\left[\vec{U}.\mathrm{CII}\right] = \frac{\partial}{\partial z}\left[K_z \frac{\partial}{\partial z}(\mathrm{CII})\right] + \left[-\mu_{\mathrm{CII}}.\mathrm{CII} + \mu_{\mathrm{CI}}.\mathrm{CI} - m_{\mathrm{CII}}.\mathrm{CII} + \frac{\partial}{\partial z}(W_{\mathrm{CII}}\mathrm{CII})\right]$	(5)
$\frac{\partial}{\partial t}(\mathrm{CVd}) + \nabla\left[\vec{U}.\mathrm{CVd}\right] = \frac{\partial}{\partial z}\left[K_z \frac{\partial}{\partial z}(\mathrm{CVd})\right] + \left[-(1-\mathrm{Diap}).\mu_{\mathrm{CVd}}.\mathrm{CVd} + \mathrm{Diap}.\mu_{\mathrm{CV}}.\mathrm{CV} - m_{\mathrm{CVd}}.\mathrm{CVd} + \frac{\partial}{\partial z}(W_{\mathrm{CVd}}\mathrm{CVd})\right]$	(6)
$\frac{\partial}{\partial t}(\mathrm{CV\ Im}) + \nabla\left[\vec{U}.\mathrm{CV\ Im}\right] = \frac{\partial}{\partial z}\left[K_z \frac{\partial}{\partial z}(\mathrm{CV\ Im})\right] + \left[\frac{(1-\mathrm{Diap})}{2}[\mu_{\mathrm{CV}}.\mathrm{CV} + \mu_{\mathrm{CVd}}.\mathrm{CVd}] - m_{\mathrm{CVIm}}.\mathrm{CV\ Im} + \frac{\partial}{\partial z}(W_{\mathrm{CV\ Im}}\mathrm{CV\ Im})\right]$	(7)
$\frac{\partial}{\partial t}(\mathrm{CVIfj}) + \nabla\left[\vec{U}.\mathrm{CVIfj}\right] = \frac{\partial}{\partial z}\left[K_z \frac{\partial}{\partial z}(\mathrm{CVIfj})\right] + \left[\frac{(1-\mathrm{Diap})}{2}[\mu_{\mathrm{CV}}.\mathrm{CV} + \mu_{\mathrm{CVd}}.\mathrm{CVd}] - \mu_{\mathrm{CVIfj}}.\mathrm{CVIfj} - m_{\mathrm{CVIfj}}.\mathrm{CVIfj} + \frac{\partial}{\partial z}(W_{\mathrm{CVIfj}}\mathrm{CVIfj})\right]$	(8)
$\frac{\partial}{\partial t}(\mathrm{CVIfm}) + \nabla\left[\vec{U}.\mathrm{CVIfm}\right] = \frac{\partial}{\partial z}\left[K_z \frac{\partial}{\partial z}(\mathrm{CVIfm})\right] + \left[\mu_{\mathrm{CVIfj}}.\mathrm{CVIfj} - m_{\mathrm{CVIfj}}.\mathrm{CVIfj} + \frac{\partial}{\partial z}(W_{\mathrm{CVIfj}}\mathrm{CVIfj})\right]$	(9)
$m_i(t) = m_i.[1 + \mathrm{Diap}(t)].[1 + (T-12)/2]$	(10)
$\mathrm{Diap}(t) = 1 - \exp\left[-50[\lvert\sin(\pi(t + \mathrm{LagT})/360)\rvert - 1]^2\right]$	(11)
$\mathrm{Spawn}(t) = [1 - \mathrm{Diap}(t)].\ \mathrm{EPR}_{\max}$	(12)
$W_i = Wm_i \tanh[\alpha(z - Z_i)]$	(13)

[a]Equations for NIII to NVI and CIII to CV are very similar to that of NII (equation (3)) and CII (equation (5)), respectively, and are not detailed further.

Table 2. Set of Common Stage-Specific Biological Parameters Used in the Simulation[a]

	Belehradek a, days	Mortality, d^{-1}	W_{max}, m h^{-1}	Z_{opt}, m
Eggs	595	0.250	–	–
NI	387	0.200	0.5	5
NII	582	0.150	0.7	5
NIII	1387	0.125	1.1	5
NIV	759	0.100	1.6	5
NV	716	0.080	2.2	5
NVI	841	0.060	2.7	5
CI	966	0.040	3.2	25
CII	1137	0.030	4.7	25
CIII	1428	0.020	6.1	25
CIV	2166	0.015	7.6	75
CV	4083	0.010	9.4	75
CVd	–	0.001	10.8	second bottom layer
CVIm	–	0.020	10.8	second bottom layer
CVI fj	–	0.010	10.8	25
CVI fm	–	0.010	10.8	25

[a]Stage-specific, temperature-dependent development time rate are computed as $D_i = a_i (T - \beta)^{\alpha}$ where $\beta = -9.11$°C and $\alpha = -2.05$. Parameters W_{max} and Z_{opt} are used to define stage-specific swimming behaviors as described in the text.

defines regional variation in the timing of the over-wintering phase, both in units of days. All the CVs were assumed to enter diapause in autumn and inversely to molt to adults in late winter/spring. The fraction of CVds exiting diapause is simply equal to (1-Diap). Laboratory experiments have shown that the final molting of diapausing CVs in adults may take 6 to 20 days, depending on food conditions and sex [*Grigg and Bardwell*, 1982]. The so-called ecdysis time varies also seasonally but tends to a mean value of ~15 days in late winter [*Grigg and Bardwell*, 1982]. High-resolution time series of population structure show a longer timescale (4 to 6 weeks) for the decrease of CVd and the peak of adult [e.g., *Diel and Tande*, 1992; *Bamstedt*, 2000]. In our model, CVs exiting diapause molt to adults with an equivalent molting time of 20 days ($\mu_{CVd} = 0.035$ d^{-1}). The spring decrease and autumn increase of the Diap function then determines the timing of the resting phase. Previous observations indicate that the active period of *C. finmarchicus* varies from late December to early June in the Gulf of Maine [*Durbin et al.*, 1997, 2000a], March to July in the Scotian Shelf [*McLaren et al.*, 2001], March to August in the Gulf of St. Lawrence [*Filteau and Tremblay*, 1953], and May to September in the Lower St. Lawrence Estuary [*Plourde and Runge*, 1993; *Plourde et al.*, 2001]. For simplicity, the lag time (lagT) was set to vary linearly with latitude on the basis of timing in the GOM (southernmost population, LagT = 30 days) and NEG (northernmost population, LagT = −60 days) in order to simulate these observed area-specific timings.

[12] Final molting to the adult stage, from either CV or CVd, was evenly distributed between female and male. Sexual maturation within CVI was assumed to take 10 days [*Plourde and Runge*, 1993], implying a sexual maturation rate for immature females of $\mu_{CVIfj} = 0.069$ d^{-1}. The spawning function, with a maximum set at 50 eggs per female per day, was assumed to be in phase with the diapausing function. The predicted range of maximal production rates between 5° and 10°C for females 2.5–3 mm in prosome length is 23–64 eggs per day [*McLaren and Leonard*, 1995]. The choice of 50 eggs per female per day is based on the median observed rate for actively reproducing populations in the study region [*Plourde and Runge*, 1993; *Runge and Plourde*, 1996]. Because the evidence for temperature dependence of egg production rate in the ambient environment is weak [*Runge and Plourde*, 1996; *Campbell and Head*, 2000a, 2000b], we assumed egg production rates were independent of temperature in the standard run.

[13] Mortality rates (Table 2) were set to decay exponentially from eggs ($m_{Eggs} = 0.25$ d^{-1}) to adults ($m_{CVI} = 0.01$ d^{-1}) at all the *C. finmarchicus* stages except CVd and CVIm (Table 2). This formulation represents a smoothed expression of observations of mortality of *C. finmarchicus* on Georges Bank [*Ohman et al.*, 2003]; note that here we have separated egg and NI mortality rates. The mortality rates at stages CVd and CVIm were set to values that were, respectively, ten-fold lower and two-fold higher than those of the active CV and females. The low mortality rates of diapausing CV (0.001 d^{-1}) is consistent with an estimate made by *McLaren et al.* [2001] on the SS over-wintering stock (0.001–0.009 d^{-1}). During the over-wintering period, the mortality rates at all the stages except CVd were set to be two-fold higher. In addition, the mortality rates were further increased over areas with water temperatures higher than 12°C (equation (10)) to eliminate an unrealistic acceleration of successive generations in warm waters, mainly in the Gulf Stream waters where actively reproducing population have never been observed [e.g.,

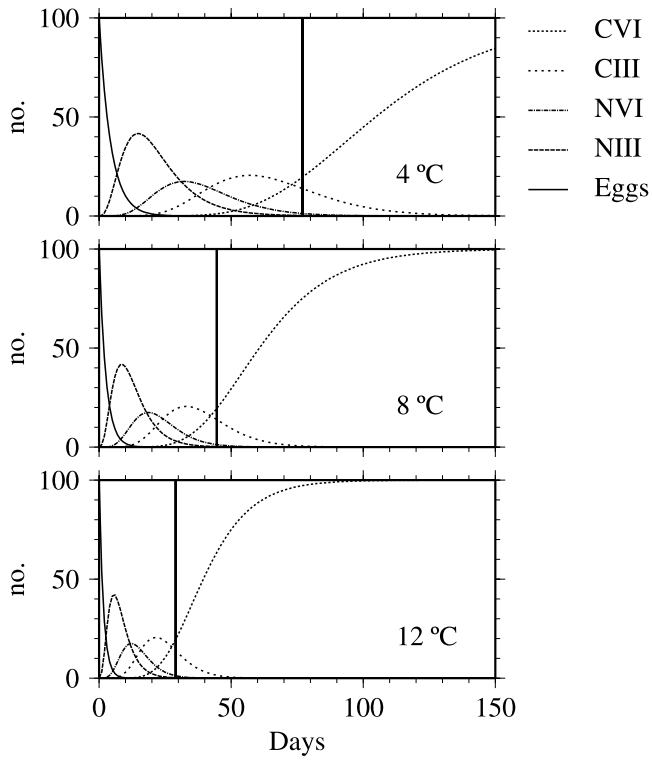

Figure 5. Single cohort development at 4°, 8°, and 12°C; each simulation starts with 100 eggs and assumes no mortality or reproduction. The bold vertical line in each panel shows the temperature-dependent development time to adult as predicted by the Belehradek function.

Planque and Batten, 2000]. This is supported by laboratory observations showing increasing mortality in naupliar and early copepodid stages at temperatures higher than 12°C (J. Runge and I. McLaren, unpublished observations, 1998). As unrealistic mortality rates may lead to a continuously decreasing or increasing population, we verified that the set of mortality rates we used gave stable populations in multi-year 1D simulations (not shown) for the LSLE, Gulf and SS temperature regimes (as on Figure 3); that is, the annual cycle and over-wintering stock are conserved from year to year.

[14] Given the vertical current shears in the GSL-SS system [e.g., *Koutitonsky and Bugden*, 1991], vertical ontogenic migration of *C. finmarchicus* may be of first-order importance for the estimation of transport between sub-areas of the system. Vertical distribution also specifies the temperature conditions experienced by the organisms during their development. We include this constraint by the use of a formulation for stage-specific swimming behavior and vertical distribution, in which vertical swimming speed is expressed in terms of stage-specific preferential depths (Z_{opt}) and stage-specific maximum swimming velocities (W_{max}), as $W_{swim} = W_{max} \tanh [\alpha(z - Zopt)]$ [*Zakardjian et al.*, 1999]. In this formulation, *C. finmarchicus* swims downward from the surface and upward from the bottom toward its specified preferential (optimal) depth. The parameter α in this formulation controls the decrease of the swimming velocities near the optimal depth Z_{opt}. W_{max} for each stage is set to one body length (BL) per second, which is sufficient for late copepodids to achieve known ontogenetic migration rates [*Zakardjian et al.*, 1999].

[15] Table 2 lists the values of Z_{opt} for each *C. finmarchicus* stage. These values were estimated from the observed spring and summer vertical distributions in the GSL [*Plourde et al.*, 2001; J. Runge et al., unpublished data, 2003]. For females, the preferential depth was set at 25 m, and for males and CVd, the preferential depth was set to the center of the layer immediately above the bottom layer. This allows the CVd and males to be distributed in a deep layer (500–600 m) on the shelf slope, as observed in the northeast Atlantic [e.g., *Heath et al.*, 2000], but without significant accumulation in the deeper layer. For all stages other than CVd and CVIm, if the bottom is locally less than the standard Z_{opt}, the preferential depth is changed to be the middle of the bottom layer. Note that only the ontogenetic migration is considered in this paper. Diel vertical migration behavior of *C. finmarchicus*, however, could readily be incorporated as more data become available.

2.3. Coupling the *C. finmarchicus* Life Model to the 3D CANDIE Temperature and Currents

[16] The main feature of the physical-biological model used in this study is the coupling of the stage-based *C. finmarchicus* life-history model to the 3D, time-varying circulation and temperature fields produced by the CANDIE physical model. The physical-biological model has the same horizontal and vertical resolutions as CANDIE, but is limited only to the top 13 levels (top 750 m). A semi-implicit Crank-Nicolson numerical scheme derived from the control-volume approach (CVA [see *Roache*, 1976]) was used to solve the set of differential equations shown in Table 1, with the Choleski's double-scanning method (or Thomas algorithm [see *Roache*, 1976]) in the alternate direction. To close the system, an iterative procedure was used to equate the derived abundance of mature females from equation (9) to the abundance of mature females used in the egg equation (1). Horizontal mixing was not considered in the model equation because we assume that the system is advection-dominated. Hence the small amount of horizontal mixing introduced by the discrete scheme for advection we used is already sufficient.

[17] We did not consider the turbulent diffusivity from the CANDIE model because the swimming ability of marine planktonic copepods is typically higher than turbulent velocity fluctuations; hence copepod movement is, in general, independent of oceanic turbulent activity in the upper ocean [*Yamazaki and Squires*, 1996]. The swimming behavior of marine zooplankton, however, is often nonlinear and multi-directional [e.g., *Paffenhöfer et al.*, 1996] in response to external and internal factors such as food availability, gut fullness, presence of predators, etc. As discussed by *Zakardjian et al.* [1999] these factors would act on individuals as dispersion functions and can be introduced as a biological diffusivity. This approach is implicitly used by *Wroblewski* [1982] in his modeling study of *Calanus marshallae* in the Oregon upwelling zone where he used a ten-fold higher diffusivity coefficient (86.4 $m^2\ d^{-1}$ instead of 8.64 $m^2\ d^{-1}$) for swimming copepodite stages in order to avoid unrealistic aggregation. We followed the same approach and the vertical diffusion in the transport equations (1)–(9) was set uniformly to 100 $m^2\ d^{-1}$ in order to avoid unrealistic aggregation of animals around their preferential depth.

[18] The vertical boundary conditions for the concentrations are zero fluxes at the sea surface and at the boundary between sea and land grid points. The lateral and bottom open-boundary conditions are Dirichlet conditions with zero concentrations for all the stages, i.e., no animals at depth greater than 750 m and no import from the Labrador Sea, mid-Atlantic bight, and the North Atlantic at large. At each time step, the physical-biological model calculates the fluxes through the open boundaries, spatially integrated total abundance, total spawning production, and mortality. A comparison of total abundance with the balance-sheet of the boundary fluxes, total spawning production, and mortality was used to check the accuracy of numerical integration. The typical relative errors, normalized by the change in total abundance, were found to be on the order of 10^{-6} for the results presented in this paper. Note that the relative errors were largely dependent on the threshold value (10^{-3} in this study) used to test the convergence of the solutions calculated in the alternate directions at each time step. A finer threshold improved slightly the accuracy of numerical results, but greatly increased the computation time without much change in results. Last, we verified that the open bottom boundary off the shelf break was not subject to a significant loss of organisms, as the swimming behavior imposed for CVd and male prevents accumulation in the deeper layer.

3. Results

3.1. Simulated Distribution and Abundance of *C. finmarchicus*: The Climatological Run

[19] The physical-biological model was initialized with a spatially uniform, shelf-diapausing CV population on

28 October, a time when all the sub-populations in the study region are assumed to be in diapause. The initial CVd concentration was set to 30 per cubic meter for water depths of less than 1000 m and zero elsewhere. The depth-integrated abundance in early January (Figure 6) reflects the continuing diapause of the initial *C. finmarchicus* sub-populations from October to December throughout the region. CVd are concentrated mainly in the deeper areas of the shelf, including the Laurentian Channel and its branches in the GSL, shelf break and SS deep basins. The higher depth-integrated abundance in the deeper areas at this time results largely from the initial conditions of the spatially uniform initial CVd concentrations, but the ability of CVd to migrate toward its deep preferential depth further reinforces these patterns.

[20] From January to March, the total *C. finmarchicus* abundance does not change much in the GSL, but increases greatly in the GOM and then later on the SS, due primarily to early arousal and spawning by the local populations. Over the western SS and GOM, the total *C. finmarchicus* abundance reaches a maximum in May and gradually decreases after July. In contrast, the total abundance in the GSL reaches a maximum in July and decreases gradually after September to near-initial values. Slightly higher over-wintering CV abundances remain in the SG and GOM, for reasons to be discussed below.

[21] The simulation predicts relatively high *C. finmarchicus* abundance in spring and summer in the deep waters off the SS and GOM. This area was initially empty of animals and is populated by the immigration at depth of the initial CVd population that drifts eastward to the southeast boundary of the model and offshore (Figure 6, January 6). A significant portion of these diapausing CVs, which originated along the shelf break or in the deep areas of the Laurentian Channel, becomes trapped in this offshore region due to re-circulation between the Labrador Current and the Gulf Stream. After arousal, females ascend to the surface layers and are dispersed northward to the slope-water region, where water temperatures are favorable for rapid growth of the spring generation.

[22] Vertical distributions of stage-grouped abundance at different locations along a north-south transect at roughly 63°W on 16 May (Figure 7) reflect their stage-specific preferential depth and swimming behavior. Eggs and weakly mobile early naupliar are distributed in the top 60 m with a slight mode around 25 m whereas later naupliar (NIII–NVI) and early copepodids (CI–CIII) aggregate for the most part near sea surface and around 25 m, respectively. The CIV–CV abundance has two modes in the vertical, one near 75 m for active animals and the other at depth for diapausing individuals. The high abundance between 500 and 600 m in offshore waters consists mostly of diapausing CV while onshore the depth of CVd abundance maximum is limited by the bathymetry. The adults also have two modes in the vertical: one near the surface for females and the other at depth for males.

[23] The predicted seasonal variation in stage structure and mean abundance (Figure 8) is generally consistent with knowledge of *C. finmarchicus* life cycles in the region (detailed comparison in the next section). The CVd of the initial generation (G_0) exits from diapause, molts to adult, and starts to spawn to produce the new generation (G_1) in January in the GOM, February in the SS, late March in the SG (southern GSL), April in the NWG (northwestern GSL), and May–June in the LSLE and NEG (northeastern GSL), respectively. The active season of *C. finmarchicus* ends with the increase of the CVd stocks and disappearance of the naupliar and early copepodids in June–July in the GOM, July–August in the SS, August in the SG and CG, and August–September in LSLE, NWG, and NEG, respectively. Figure 8 also shows a second generation (G_2) produced by a small fraction of adults of (G_1) at the end of the first-year reproduction in these sub-areas. However, recruitment of diapausing CV's was made up mostly of G_1. The model results also correctly simulate that CVd and females dominate during the period from late fall to late winter or early spring, with their over-wintering abundance slightly decreasing gradually with time.

[24] The depth-integrated CVd abundance over the eight sub-areas at days 30 and 390 (Table 3) are representative of the over-wintering stocks initially and at the end of the 1-year simulation. Over the SS and in the deeper areas of the GSL (i.e., LSLE, NWG, CG, and NEG), the over-wintering stocks at day 390 are very similar to the initial concentrations, despite very different environmental conditions (timing of diapause, temperature and circulation) prevailing in those sub-areas. In the GOM and SG, however, the over-wintering stocks at day 390 are much higher than the initial conditions, although they are in the range of observed values for the GOM [e.g., *Durbin et al.*, 2000a]. The increased population in the GOM is in response in part to rapid development times at the relatively high ambient temperatures and in part from continuous imports of *C. finmarchicus* from the SS and the adjacent shelf break in the Nova Scotia and Labrador Currents, as shown below. The increase of the over-wintering stocks in the SG region, on the other hand, is principally the result of an inadequate formulation of the swimming behavior of deep-dwelling stages CIV–V in shallow water <75 m, in which the preferred depth is forced to be the middle of the bottom layer. Since the currents at this depth are relatively weak due to bottom friction, the deep-dwelling stages are unable to escape from these shallow areas and would likely be subjected to higher mortality rates, a factor not included in the present model. In the Laurentian Channel, the 70% decrease in simulated over-wintering stock (Table 3) is likely due to the absence of immigration of *C. finmarchicus* from the Labrador and Newfoundland shelves through the eastern open boundary, which was set at zero in this study.

3.2. Comparison With Observed Life-History and Abundance

[25] The results of the climatological run are compared to four different data sets describing the annual life cycle of *C. finmarchicus* in the study region. The first data set derives from a monitoring program in the LSLE in which a fixed station 330 m deep located 16 km north of Rimouski was visited each week from May to November in 1994, 1996, and 1997 [*Plourde et al.*, 2001]. Eggs were not enumerated from preserved samples, and older naupliar stages (clearly identified as *C. finmarchicus*) and younger copepodid stages were grouped as NIII–VI and CI–III, respectively. The second data set originates from a field study conducted between 1945 and 1949 in the Baie des

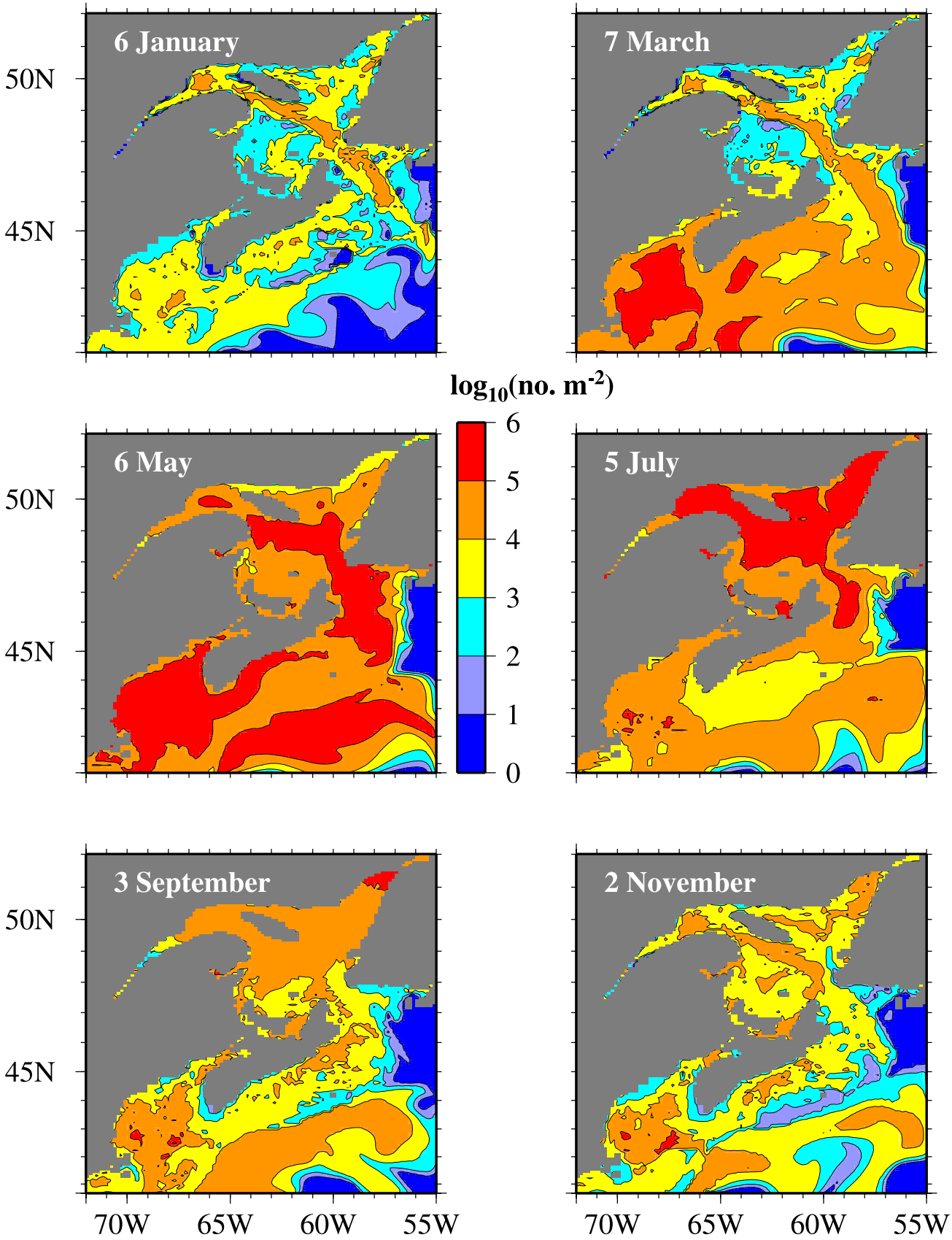

Figure 6. Seasonal trends of the total *C. finmarchicus* population plotted as log10 of depth-integrated abundance over the 1-year simulation.

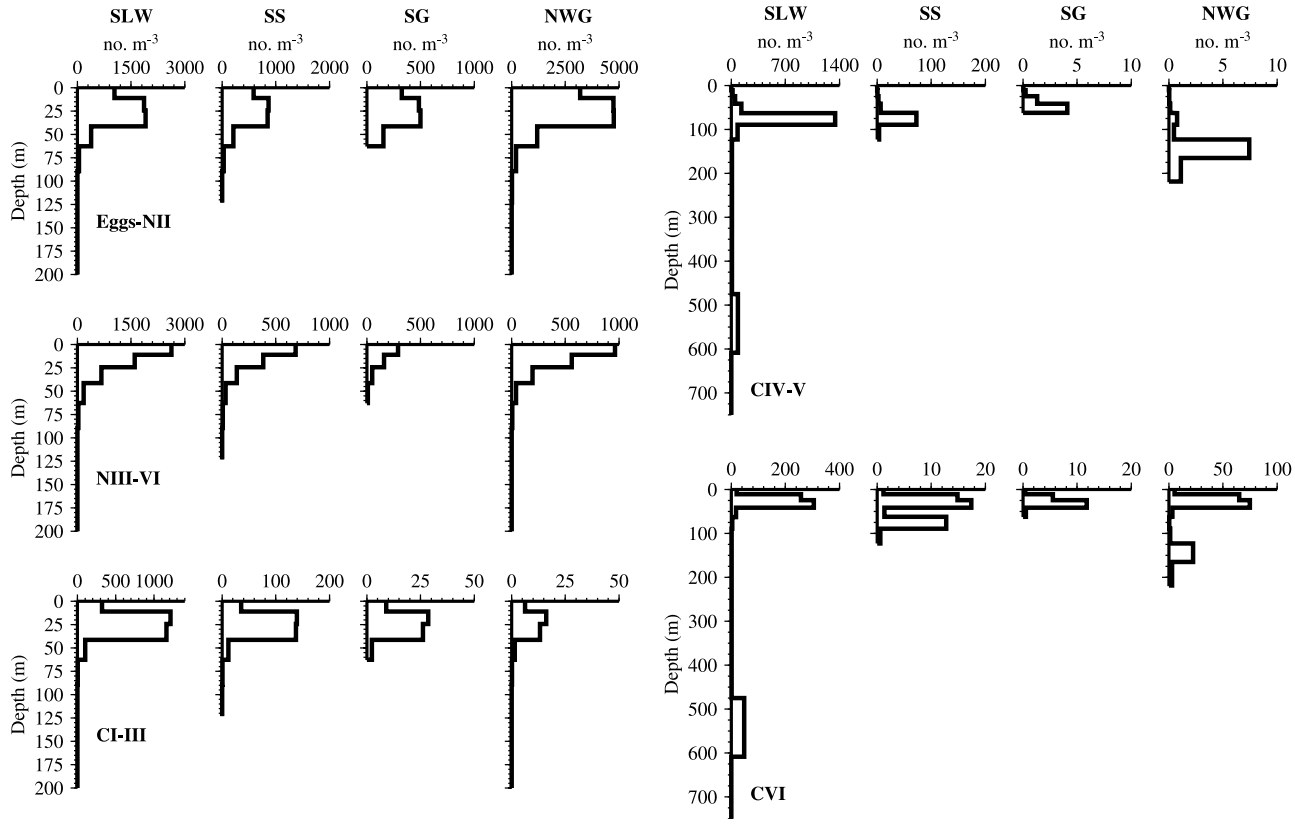

Figure 7. Vertical distributions of eggs to NII, NIII–VI, CI–III, CIV–V, and adults of *C. finmarchicus* at different locations along a south-north section (63°W) extracted at day 200 of the simulation (May 16). Only the upper 200 m is shown for the young stages (e.g., gs-CIII). The depth axis is reduced in shallow areas. Note change in abundance scale among regions.

Chaleurs (SG) at a sampling site 7 km south of Grande Rivière [*Filteau and Tremblay*, 1953]. All *C. finmarchicus* stages except eggs were counted; we calculated the mean stage abundance from these data. The third data set represents detailed observations gathered in Bonne Bay [*Starr et al.*, 1994; M. Starr, unpublished data, 1994], a deep fjord on the western shore of Newfoundland in the northern Gulf of St. Lawrence (NEG). The fourth data set, representative of the SS, was obtained from (1) monthly plankton samples collected between March 1991 and March 1992 during the Ocean Production Enhancement Network (OPEN) program on and around Western Bank, (2) plankton hauls in 1995–1996 from seven stations on the "Halifax transect" across Emerald Basin to deep water beyond the shelf break, and (3) plankton samples from Emerald Basin between 1984 and 1992. Sample collection and analysis are described in *McLaren et al.* [2001]. We calculated depth-integrated abundance (number per square meter) from mean concentration (number per cubic meter) by assuming a mean shelf depth of 75 m.

[26] Figure 8 summarizes the comparison with the model results. In the LSLE, the simulated life cycle, particularly the seasonal trend in stage-structure, agrees reasonably well with the data and the model reproduces the right order of relative abundance of CV and CVIf during the period of reproduction. However, the simulated reproduction begins about 1 month earlier than observed and the modeled abundance of early life stages does show the persistence into late summer and autumn as seen in the observations.

[27] In the SG, the timing of the observed maximum of CI–CIII in June and the increase of CV in late summer are consistent with the observations. The model results overestimate the abundance of CIV–V and adults in this area but underestimate the relative abundance of early stages in late summer and autumn. Note that the simulated life cycle and abundance in Figure 8 represents a mean for the entire southern Gulf whereas the station used by *Filteau and Tremblay* [1953] was situated in relatively shallow water (76 m) near the coast. Over this shallow water area, the input of G_0 females from arousal of the over-wintering stock in deeper water of the Laurentian channel should depend on local circulation, including input from the coastal jet rounding the Gaspé Peninsula. Because the spatial resolution of the model is too large to resolve the details of the nearshore

Figure 8. (opposite) (left panels) Simulated mean abundance and stage structure of *C. finmarchicus* in each sub-area (abbreviations as in Figure 1) compared with (right panels, except GOM) observations in that sub-area. Log absolute abundance is shown for stages NIII–NVI (CI–CIII in NEG), total CV, and adult females. Stage structure is expressed as percent of the population between Nauplius III to adults. Both legends appear at bottom right.

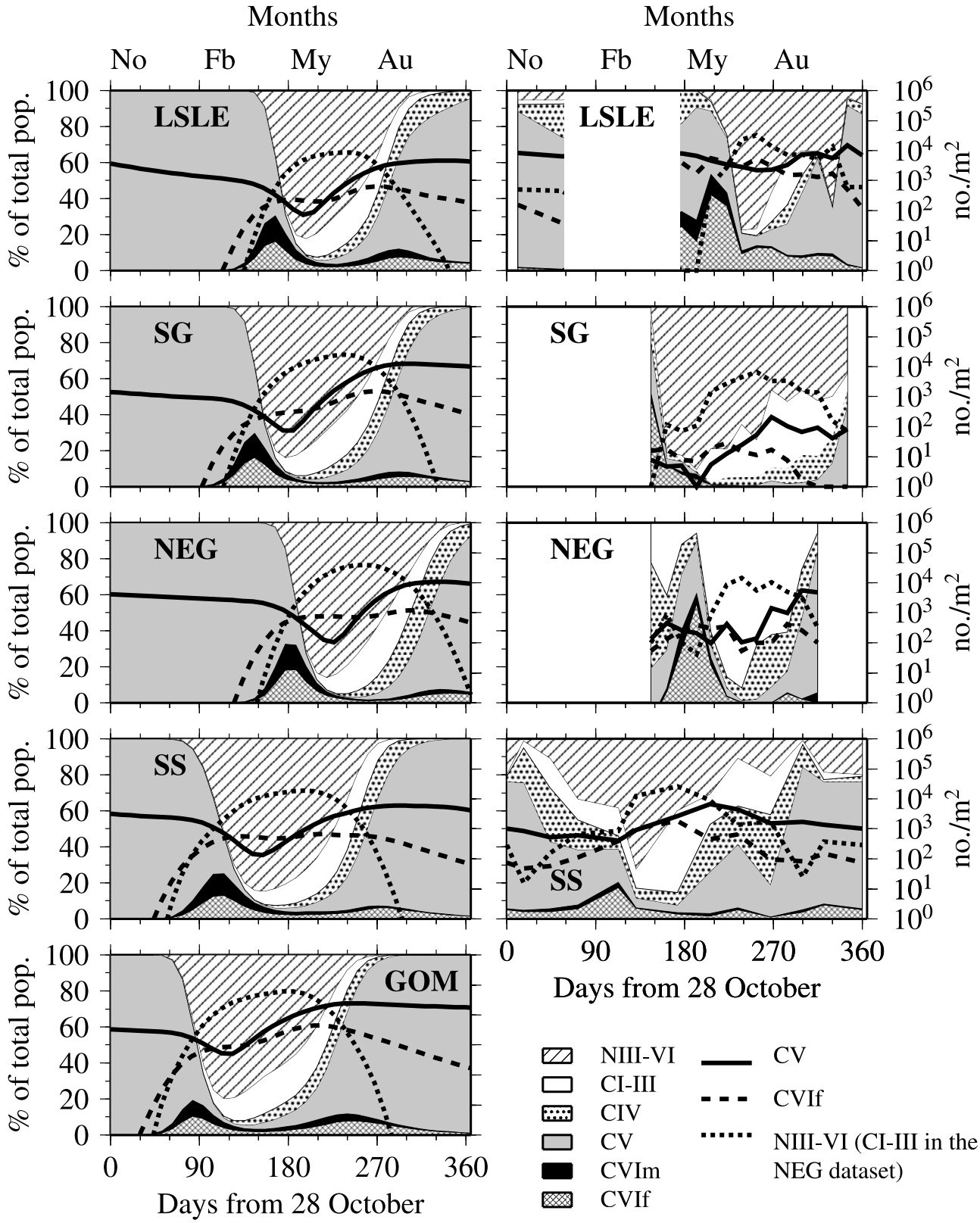
Months
No
Fb
My
Au
LSLE
SG
NEG
SS
GOM
% of total pop.
no./m2
Days from 28 October
0
90
180
270
360
NIII-VI
CI-III
CIV
CV
CVIm
CVIf
CV
CVIf
NIII-VI (CI-III in the NEG dataset)

Table 3. Mean Abundance (number per m^{-2}) of the Overwintering Stocks After 30 and 390 Days of Simulation by Areas Defined in Figure 1

Area	Day 30	Day 390
LSLE	2845	2951
NWG	6729	7627
NEG	3837	7027
SG	3976	8652
CG	6644	9037
LC	7278	2237
SS	3977	3197
GOM	3066	16261

circulation where the sampling station was located, the location of the *Filteau and Tremblay* [1953] study site in itself could account for differences between the model and the observations in the early life stages and females.

[28] In the NEG, the simulated CV and CVIf abundance and the timing and duration of seasonal production agree reasonably well with the Bonne Bay observations (the naupliar stages were not counted and hence do not show up in the observed stage structure). The NEG data were used to set the coefficients in the general equation describing latitudinal variation in the reproductively active season (equation (11) in Table 1); hence the simulation of the timing of the life cycle in this area is not strictly independent of the empirical data. The simulated percentages of stage CI–IV in the NEG are however much lower than the observations at the beginning of the spawning season. The Bonne Bay sampling station was in the fjord's external basin, which connects to the GSL across a shallow sill about 50 m deep. The marked contrast between the very low adult abundance and very high abundance of early copepodids in summer suggests imports of *Calanus* from neighboring open waters where the winter resting stock of *C. finmarchicus* resides. The physical model would not provide fine-scale simulations of water exchange between the external basin and the neighboring open waters. Moreover, similarly to the SG data set, as the modeled life-cycle represents a mean for the entire northeast Gulf, the sampling location of the Bonne Bay data set contributes to discrepancies between simulated and observed *C. finmarchicus* abundance.

[29] On the SS, there is good agreement in the timing of maximum relative abundance of adults in mid-February and maximum absolute abundance of naupliar and stages CI-CIII between mid-March and mid-April. The decline in naupliar abundance in summer, between June and mid-August, is simulated. However, the model indicates no naupliar stages present in September, whereas the observations show persistence of early life stages throughout the year (although at levels 2 orders of magnitude less than the spring). The generation originating from the March–August spawning is the main contributor to recruitment of the overwintering stocks in the simulation.

3.3. Flux Estimates and Impacts on Area Budgets

[30] To evaluate the importance of horizontal exchange relative to local *C. finmarchicus* population dynamics, we calculated the cross-boundary fluxes of abundance across the 10 regional boundaries shown in Figure 1, LSLE/NWG, NWG/CG, NEG/CG, SG/CG, CG/LC, eastern LC, southern LC, LC/SS, southern SS, and SS/GOM (Figure 9) and compared the corresponding annual sum to the annual total net production in each area (Table 4). The total net production is defined here as the difference between the total egg production and total mortality of all life history stages (including eggs). For all the areas identified in Figure 1, except the NWG, where the net flux is negligible, the annual net fluxes are 17 to 40% of an area's net production (Table 4), suggesting that transport of *C. finmarchicus* is of first-order importance for the GSL-SS stock. The cross-boundary fluxes are for the main part due to the transport of young stages. This is due to the greater abundance of young stages and higher surface current velocities, although deep-dwelling stages (CIV–V and CVd) can also be subject to strong transport (Figures 9a, 9b, and 9j).

[31] The flux across the LSLE/NWG boundary plays a very minor role in the NWG, where it is no more than 2% of annual mean net production. Conversely, it is important in the LSLE budget (18.2%). Stage-specific fluxes across the LSLE boundary (Figure 9a) are globally consistent with the prevailing estuarine-like circulation in spring. Surface-dwelling stages (eggs, nauplii, and females) are flushed from the estuary in spring/early summer while deeper-dwelling stages (CI–V) are imported from the NWG later. Nevertheless, the flows of eggs and stages NI–II reverse in summer due to the combination of (1) a different vertical distribution than NIII–VI (Figure 7), (2) a greater *C. finmarchicus* abundance in the NWG, and (3) a gyre-like circulation that sets up seasonally in the transition region between the LSLE and NWG (Figure 4) as described by *El-Sabh* [1979], *Koutitonsky* [1979], and *Ingram and El-Sabh* [1990]. As the annual flux is cumulative across stages, stage-specific differential transports compensate, with a final balance sheet showing net import into the LSLE. Hence, while there is flushing of early life stages from the LSLE in late spring and early summer, our model results show that this transport is not significant to the NWG production. While the LSLE/NWG boundary surface is relatively insignificant compared to the large surface area of the NWG, it is important compared to the much smaller surface area of the LSLE.

[32] The seasonal and stage-specific variability of the calculated fluxes between NWG and CG (Figure 9b) is due to a strongly sheared circulation between the Gaspé Coast and Anticosti Island that results from the adjustment of two cyclonic gyres occurring north (the NWG Gyre) and south (the CG Gyre) of the Gaspé-Anticosti channel (Figure 4). The surface circulation is downstream to the west and near the center of the Laurentian Channel (the Gaspé Current) and upstream east of the channel. At greater depths (>25 m), upstream-east currents prevail, but the mean circulation again reverses at depths >150 m. In spring and summer, there is a net upstream flux of eggs, early naupliar stages (NI–NII), and early copepodids (CI–CIII) from the CG to the northwestern NWG, but there is a slight net downstream flux in late summer. In contrast, NIII–VI are continuously exported to the CG, from late spring to early autumn, due again to their marked aggregation in the surface layer. Diapausing CV and males, on the other hand, are always exported from the NWG to the CG, while intermediate deep-dwelling stages (CIV and active CV) are transported from the CG to the NWG. Again stage-

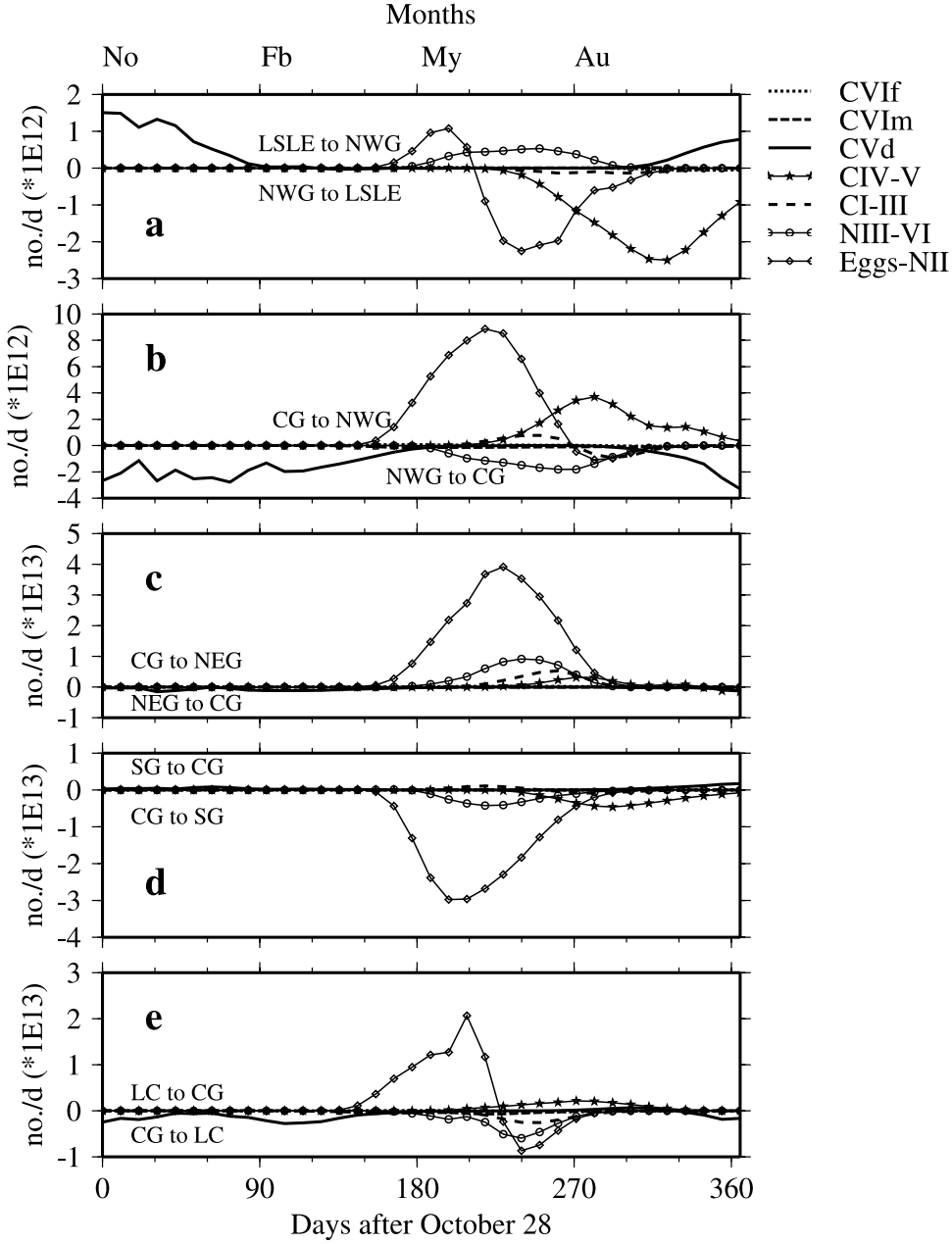

Figure 9. Seasonal variations of stage-grouped transport across the ten boundaries shown Figure 1: (a) LSLE/NWG, (b) NWG/CG, (c) NEG/CG, (d) SG/CG, (e) CG/LC, (f) east LC, (g) SS/LC, (h) SS/GOM, (i) south LC, and south (j) SS. For each panel the direction of the transport (depending on sign) is indicated.

specific and seasonal variations lead to a low annually cumulative value that is slightly positive (+1.6%) for the NWG budget and not significant for the CG (<1%).

[33] Calculated fluxes between NEG and CG show a net export from the CG to the NEG for all stages except CVd and males (Figure 9c), with annual sum about 10–20% of the two areas' budgets. Transports are generally in agreement with the known circulation in the northeastern part of the Gulf [e.g., *Koutitonsky and Bugden*, 1991]: a mainly cyclonic surface circulation with a much more marked northward component along the west coast of Newfoundland (Figure 4) and a reversed net flow at depth (>100 m). Hence eggs, nauplii, and early copepodids (CI–CIV) move northeastward from the CG to the NEG, with maximum fluxes in June for eggs and naupliar and in July August for the early copepodids. In contrast, there is a constant southwestward flux of the deep-dwelling, diapausing CV and of adult males from the NEG to the CG; however, the surface northeast fluxes dominate and the balance sheet is mainly an export from the CG to the NEG.

[34] The annual cumulative transport across the SG/CG boundary shows a net import to the SG from the CG which is ~17% of the SG annual net production but is not as important to the CG budget (8%). The transport is domi-

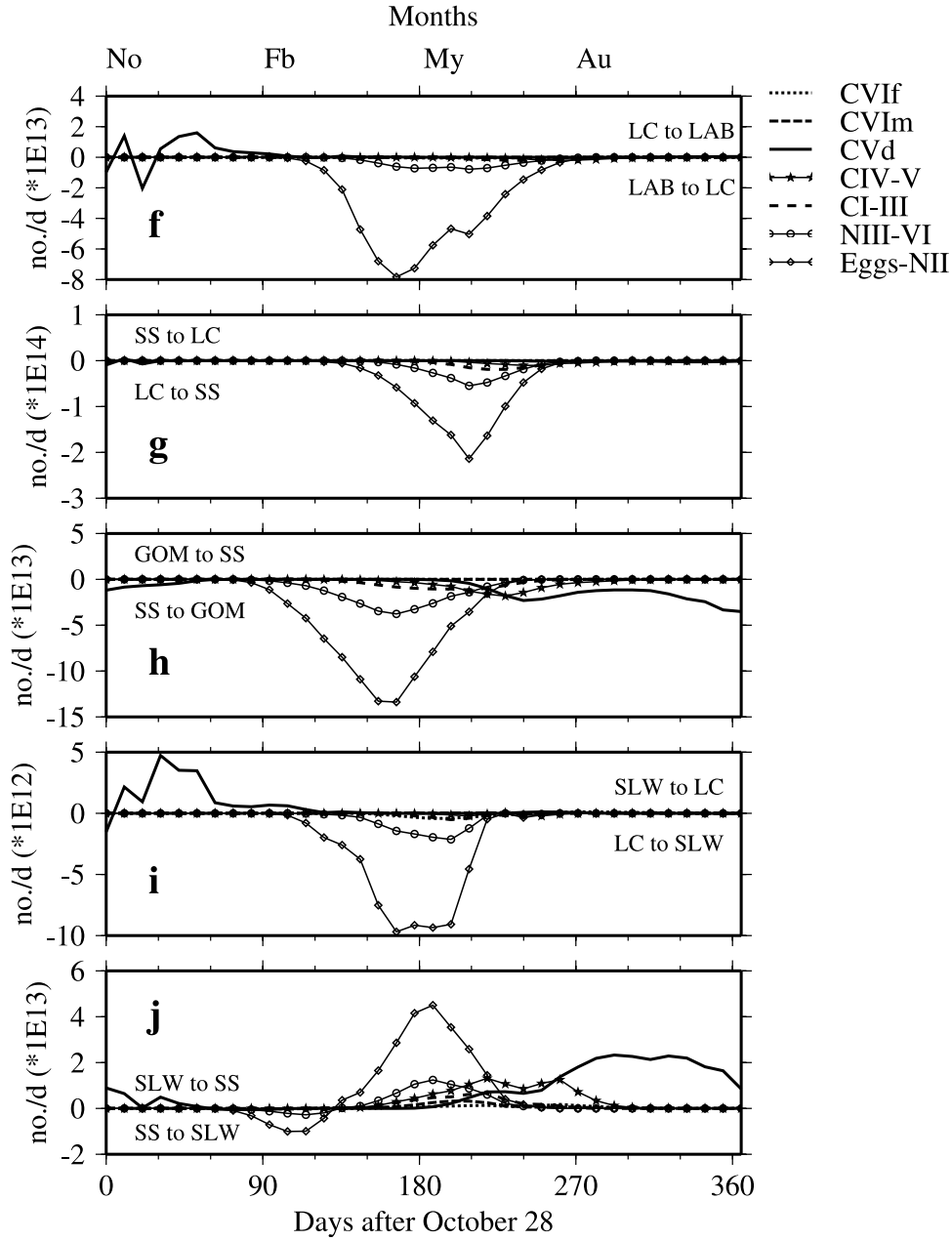

Figure 9. (continued)

nated by a constant import of eggs and naupliar stages from the CG to the SG, whereas transport of older stages is more seasonally variable (Figure 9d). The inflow of young stages is mainly from transport by the Gaspé Current and the CG cyclonic gyre. Outflow from the eastern side of the SG results in a net outward flux of CI–CIII in early summer and diapausing CV are always exported from the SG, but both at a low rates.

[35] The cumulative annual transport across Cabot Strait accounts for only 0.2 and 2% of the CG and LC annual net production, respectively. The circulation in Cabot Strait is strongly sheared and shows marked seasonal variations that explain this low relative exchange across all life history stages. The computed fluxes show a strong transport into the GSL of naupliar stages in May–June which reverses in July–August (Figure 9e). The May–June peak results from the surface inflow of LC population along the northern side of Cabot Strait. There is a summer outflow of copepodid stages C1–C3, which is consistent with previous findings showing high concentrations of stages C1–C3 near the entrance to the Gulf of St. Lawrence in June [*Sameoto and Herman*, 1992]. In winter and spring, there is a net transport of deep-dwelling stages (CIV–CV and males) from the CG to the LC whereas in summer the same stages are transported into the GSL from the south.

[36] Fluxes in the LC, SS, and GOM show a net southwestward transport of all stages of *C. finmarchicus* from the Newfoundland Shelf to the LC and along the SS to the GOM, reflecting the residual circulation of the Labrador Current along the shelf break and of the Nova Scotia

Table 4. Magnitude of Annual Cumulative Boundary Fluxes Relative to Net Production in Each Sub-Area[a]

		LSLE	NWG	NEG	SG	CG	LC	SS
TEP		7.95E + 14	1.23E + 16	1.83E + 16	9.45E + 15	2.78E + 16	2.16E + 16	2.21E + 16
TM		−6.57E + 14	−1.11E + 16	−1.65E + 16	−8.07E + 15	−2.48E + 16	−1.93E + 16	−1.97E + 16
NP		1.39E + 14	1.28E + 15	1.81E + 15	1.38E + 15	3.01E + 15	2.31E + 15	2.44E + 15
Yearly cumulated flux								
LSLE/NWG	−2.39E + 13	**+0.172**	**−0.019**					
NWG/CG	1.99E + 13		**+0.016**			**−0.007**		
NEG/CG	3.28E + 14			**+0.181**		**−0.109**		
SG/CG	−2.42E + 14				**+0.176**	**−0.080**		
LC/CG	−5.81E + 12					**−0.002**	**+0.003**	
East LC	−5.97E + 14						**+0.259**	
South LC	−5.62E + 13						**−0.024**	
LC/SS	−1.50E + 15						**−0.651**	**+0.615**
South SS	6.82E + 14							**+0.280**
SS/GOM	−1.67E + 15							**−0.684**
Balance		+0.172	−0.003	+0.181	+0.176	−0.198	−0.414	+0.211

[a]See Figure 1. Column headings indicate sub-area. The first three rows show total egg production (TEP), total mortality (TM), and net production (NP) for each sub-area as number per year (no. yr $^{-1}$). Annual cumulative fluxes (no. yr $^{-1}$) are provided in row 4. Subsequent row headings indicate location of boundary flux. Bold numbers give proportion of annual cumulative flux relative to NP for each sub-area and boundary (positive and negative values indicate import and export, respectively). Bottom row shows the overall balance of annual flux/NP for each sub-area.

Current over the inner Scotian Shelf (Figures 9f–9h). The southwestward annual transport is about 26% of the LC annual net production but more than 60% of SS annual net production, which includes both the import from the LC and the export to the GOM. The exchange with slope water through the LC south boundary is low (less than 3% of the annual net production) but is much more marked on the SS shelf-break. Transport is mainly out of LC for all stages (Figure 9i), except for import of CVd in winter, which may be an artifact of the spin-up from initial conditions. Along the SS south boundary, there is more seasonal variability, mostly in the fluxes of early life stages (Figure 9j), because the Labrador Current follows the shelf break and fluctuates seasonally in overlap with the boundary. The model predicts an outward flux of early life stages (eggs to NVI) in late winter and then a reversal and substantially higher input of early life stages onto the SS in April–June. Older copepodid stages (CIV–CV) are transported in large numbers onto the SS in summer and autumn, in particular a massive import of CVd that reflects the abundance of the slope-water stock. The balance consequently shows a significant import from the slope water that contributes about 28% of the SS annual net production.

4. Discussion

[37] Our objective in this study was to estimate the relative importance of transport in relation to biological production in sub-areas of the GSL and SS. For that purpose, we used a simplified stage-based model that focused on vertical distribution, advection-induced mixing of sub-populations in a large-scale model, and estimation of the resulting fluxes. We did not focus on individual growth as we were concerned here with first-order biophysical influences on numbers of *C. finmarchicus* rather than biomass. Although our mathematical model differs from more detailed life-history models, such as age-within-stage models, the model we present here yielded a realistic ontogeny and annual abundance pattern, i.e., a cascading of the population through eggs to adults with consistently lower abundance, by an order of magnitude or more, from eggs and naupliar to copepodids as in previous modeling studies [e.g., *Tande and Slagstad*, 1992; *Miller and Tande*, 1993; *Carlotti and Radach*, 1996]. The resemblance of the simulated and observed life stage abundance and a final CVd population similar in abundance to the initial population and with a realistic distribution, show the ability of this simplified model to simulate a mean climatological state of the populations of *C. finmarchicus* in the eastern Canadian waters. As both the seasonal evolution of abundance and circulation are reasonably represented in the model, we argue that it captures, within the right order of magnitude, the relative importance of transport in relation to biological production.

[38] It is recognized that this simplified stage-based approach does not include aspects of *C. finmarchicus* population dynamics that may have a significant, although we believe second-order, influence on results of the simulations. First, our simplified model does not explicitly account for variability in the availability of food resources that would influence development and reproduction during the active season. While development in *Calanus* is less influenced than growth rate by food [e.g., *Vidal*, 1980; *Campbell et al.*, 2001b], there is the possibility, not considered in our model simulations, that development during the active season may be retarded during low chlorophyll, post-bloom periods [e.g., *Campbell et al.*, 2001a]. This may explain, for example, a mismatch between predicted and observed development rates on Western Bank on the SS during late spring [*McLaren et al.*, 2001]. Likewise, we used here a "climatological mean" state of reproduction of *C. finmarchicus* during the active season with a constant rate of 50 eggs female^{-1} d^{-1}, the median rate of egg production from observations in the Gulf of St. Lawrence [*Runge and Plourde*, 1996]. Empirical studies indicate that *C. finmarchicus* in this system is capable of sustaining egg production not only during periods of high phytoplankton biomass but also during the low-chlorophyll, post-bloom period [*Ohman and Runge*, 1994; *Runge and de Lafontaine*, 1996]. We believe that food limitation is not of first order for a climatological view of the system but would be fundamental for subsequent studies on interannual or inter-

decadal variability. As data become available, future model versions will explore the sensitivity of the annual patterns of *C. finmarchicus* abundance and distribution to food-limited reproduction that may occur at particular times in different areas of the system.

[39] Mortality is stage-specific and varies in time and space with temperature or ecological conditions [e.g., *Ohman and Hirche*, 2001; *Ohman et al.*, 2003; *McLaren et al.*, 2001] and consequently may deviate from the single mortality schedule that we applied to all areas. An alternative approach is to use area-specific mortality rates since ecological conditions obviously differ between the GOM and GSL with respect to temperature, food limitation [e.g., *Durbin et al.*, 2000a; *Campbell et al.*, 2001a] and, undoubtedly, predator fields. In the coupled model of *C. finmarchicus* dynamics on Georges Bank, *Miller et al.* [1998] had to impose higher mortality rates on the simulated second generation (G2) in order to scale the overall development of the population. *Lynch et al.* [1998] found it necessary to delay or temporarily limit G1 reproduction, by invoking food limitation, in order to scale the development of G2. The closure of biological models by mortality is not a new problem in ecological modeling [e.g., *Edwards and Yool*, 2000] but there is no ideal solution for this problem at this time because information on temporal and spatial variability of *C. finmarchicus* mortality is too sparse to permit a deterministic parameterization of mortality. We applied a uniform mortality regime over the entire region so that differences in simulated life cycles and abundance were therefore only due to the effects of circulation and temperature prevailing in each of the sub-areas.

[40] A major problem in modeling the population dynamics of *C. finmarchicus* is the quantitative description of the over-wintering phase of the seasonal life cycle. In our model it is assumed that the life cycle of *C. finmarchicus* is driven by an optimal window for reproduction outside of which the population waits in a dormant phase for favorable conditions. This is done by imposing a seasonality function that determines the time window during which the sub-populations emerge from diapause and spawn and within which the temperature-dependent molting rates and stage-specific mortality rates drive the population growth rate. This formulation captures the main patterns of the life cycle of *C. finmarchicus* off eastern Canada including the importance of seasonality as a major driving factor for its dynamics. We have based the area-specific seasonality functions on empirical observations of life cycle timing in the GOM and NEG; hence the model simulations and field observations are not completely independent with respect to timing of reproduction. In reality, the match between the timing of arousal and the seasonal variation of environmental conditions, mainly temperature and food abundance, may crucially influence interannual variation in the dynamics of *C. finmarchicus* populations [e.g., *Hirche*, 1996a; *Head et al.*, 2000]. Here we assumed that the simulated system represents an idealized seasonal reproductive cycle for each sub-region, with no other local effects other than those due to the circulation.

[41] The simplified seasonality function defining the dormant period during which development and reproduction are dormant has the effect of limiting the simulation of the *C. finmarchicus* population to one generation per year. In general, the first generation (G1), hatched in the cold waters of spring, develops more slowly than a subsequent generation later in summer. Too short a reproduction and development window in our model would limit the development of the second generation mainly by preventing molting of G1 from CV to adults, but in addition would suppress the spawning of the small stocks of G1 females that are found in both the simulations and observations (Figure 8). One generation annually is typical in most northern populations of *C. finmarchicus* [*Tande*, 1982; *Tande and Slagstad*, 1992; *Bamstedt*, 2000; *Head et al.*, 2000], whereas in warmer waters, there are often two full generations, as on the Iceland Shelf [*Gislasson et al.*, 2000; *Gislasson and Astthorsson*, 1996], weather station India [*Irigoien*, 2000], and the GOM and Georges Bank [*Durbin et al.*, 1997, 2000a; *Meise and O'Reilly*, 1996]. The LSLE and GSL are cold environments where the one-generation scenario is generally observed [*Plourde et al.*, 2001]. *McLaren et al.* [2001] considered that two generations would be the general rule on the SS; however, they also suggest that the relative importance of the two generations for recruitment of overwintering stocks may vary in different parts of the shelf. Nevertheless, as the one generation simulated by the model gave relative and absolute abundance similar to the observations, we believe that this limitation would not strongly affect either the robustness of the estimated transports or their importance relative to the annual net production. A more refined model description of this process awaits analysis of long-time series data [e.g., *Therriault et al.*, 1998] and a better understanding of factors that drive the ontogenetic timing of entry and emergence from diapause in *C. finmarchicus* populations in the western Atlantic Ocean [*Miller et al.*, 1991; *Hirche*, 1996b; *Hind et al.*, 2000].

[42] Some physical processes were not resolved by the hydrodynamic model. First, the CANDIE model was run in diagnostic mode in which the conservation equations for temperature and salinity are not calculated. Such diagnostic calculations are robust in long-term integration, but unable to resolve the interactions of temperature and salinity with the flow field. Second, the wind stress was not used directly in the momentum equation to drive the flow. Therefore, the model results presented in this study excluded the Ekman transport and coastal upwelling events associated directly with the wind. Third, the CANDIE model generated an estuarine-like circulation in the LSLE, but did not produce the spring flushing of the surface layer in this area due to the coarse model resolution. *Zakardjian et al.* [2000] discussed the important role of flushing of the euphotic zone driven by freshwater runoff in controlling the timing of the phytoplankton bloom in the area. This flushing should also apply to surface-dwelling nauplii and females, and reinforce the delay of the *C. finmarchicus* reproduction observed in the LSLE [e.g., *Plourde et al.*, 2001]. The same constraints apply to the GOM, where small-scale circulation strongly controls *C. finmarchicus* distribution and abundance [e.g., *Hannah et al.*, 1998; *Shore et al.*, 2000]. The apparent excessive model population of *C. finmarchicus* in the GOM may partly result from too little export to Georges Bank, which leads to local trapping of *C. finmarchicus* imported from the SS. This shows the present limitation of the model for describing local-scale processes even though the regional circulation is globally well represented in CANDIE.

[43] Modeling the influence of transport and advection on *C. finmarchicus* population dynamics requires understanding of vertical distribution and migration behavior [e.g., *Hannah et al.*, 1998; *Zakardjian et al.*, 1999]. In our model the vertical distribution is stage-specific and is achieved through the imposed swimming behavior. Our model description of vertical distribution derives from observations; however, there may also be local exceptions or changes in distribution due to local environmental conditions [e.g., *Tande*, 1988]. For example, it is not clear whether deep-dwelling stages in shallow waters would be trapped on shallow areas like the SG. The shallower water likely promotes higher mortality rates in later stages, because of higher predation on the larger copepodids that cannot escape predators by migrating to deeper water. The imposed swimming behaviors of NI–NII and NIII–VI may have caused artifacts in the advection of these stages, which are generally assumed to be transported as a whole. While eggs and early naupliar are evenly distributed in the upper 50 m, the weak swimming capacity of NIII–VI allows them to aggregate in the upper surface layer, as observed by *Durbin et al.* [2000b]. In strongly vertically sheared areas, such as the LSLE, and the Gaspé-Anticosti and Cabot Straits, this slight difference in mobility and vertical distribution is enough to create different flux patterns. More empirical observations in sub-areas of the GSL-SS system are needed to increase our knowledge about swimming behavior and vertical distribution.

[44] Despite the limitations of the model in its present form, as discussed in the previous sections, the results from this climatological run serve to elaborate existing hypotheses and suggest new ones about the effects of basin-scale physical processes in the dynamics of regional *C. finmarchicus* populations. *Plourde and Runge* [1993] and *Plourde et al.* [2001] put forward the hypothesis that the Lower Estuary/Gaspé Current serves as a *Calanus "*pump,'' exporting to the GSL naupliar and copepodid stages produced in the Lower Estuary in late spring and summer. While the spatial resolution of the model does not clearly resolve the seaward circulation in the LSLE and NWG, it nevertheless shows a distinct peak in flux of early *Calanus* life stages from the LSLE to the NWG in summer and an inflow of diapausing CV into the LSLE during the winter months (Figure 9a). As discussed earlier, because of the differences in surface area of the LSLE and NWG, the influx of stage CV is relatively much more important to the LSLE than its contribution of early life stages to the NWG (Table 4). The model results, therefore, do not indicate an important role for the *Calanus "*pump'' in the dynamics of the GSL population, although the NWG/LSLE exchanges would be of first importance for the LSLE population.

[45] An important new hypothesis based on insights from the model results is that the GSL population is self-sustaining. The GSL is connected to the SS by Cabot Strait, through which surface GSL water flows out along the southwestern side and surface waters from the Newfoundland and Labrador Shelf flow in along the northeastern side. At depth, Atlantic slope water flows slowly into the GSL through the Laurentian Channel. The two inflows are thought to compensate for the outflow from the St. Lawrence. No imports from the Labrador Sea are considered in the model, so that the large influx of early naupliar stages in spring, due to the initial population in the LC area (Figure 9e), rapidly decreases and is even reversed later in summer. The inflow of deep dwelling stages (CIV–CV and males) is less than the outflow of nauplii and early copepodids. Hence the overall balance shows export (Table 4), yet the GSL maintains its own population based on its local production, without any import from the Labrador Sea.

[46] Advection is nevertheless still important to the distribution of *C. finmarchicus* within the GSL. The fluxes and budgets showed strong exchanges between GSL sub-areas, with the CG being a buffer area between the SG, NWG, and NEG. The CG seems to be the main area for *C. finmarchicus* production in the GSL and is a source for the three adjacent sub-areas; only a small export from the SG to the CG, of CI–III in June, was revealed by the calculated fluxes. The literature on *C. finmarchicus* in the GSL, like our simulated data (Figure 6), indicates highest female abundances in the CG, $\sim$6000 m^{-2} [*Runge and de Lafontaine*, 1996] [see also *de Lafontaine et al.*, 1991]. The conclusion that the CG is the main source of *C. finmarchicus* in the SG is consistent with the results of *Runge et al.* [1999], who found that *C. finmarchicus* abundance in the SG is inversely correlated to the winter-spring freshwater discharge from the St. Lawrence River system (RIVSUM). On the basis of our model results, we hypothesize that a high RIVSUM increases seaward circulation in the SG and its edge, south of the LC, hence favoring flushing of the SG and limiting the invasion of the over-wintering CG population. In a low RIVSUM year, the slower flushing of the surface layer in the SG and in the south of the LC allows more time for the CG population to invade the SG after arousal.

[47] The flux calculations show that transports arising from the mean southwesterly flow across the SS from the LC and into the GOM (Figures 9f–9h) are equivalent to about two thirds of the net annual production occurring on the shelf (Table 4). The large-scale transport from the SS to the GOM and Georges Bank is noted in earlier studies [*Meise and O'Reilly*, 1996; *Miller et al.*, 1998; *Shore et al.*, 2000]. The source of input to the SS has been the subject of several studies of *Calanus* distribution in relation to hydrographic features. *Herman et al.* [1991] concluded that the Nova Scotia Current originating from the outflow of the GSL is the major supplier of *Calanus* to the mid-Scotian shelf. They hypothesized that the copepodids transported onto the SS would accumulate in the SS basins during the seasonal ontogenetic migration in summer and autumn. *Sameoto and Herman* [1992] suggested that there are three sources of *C. finmarchicus* found on the SS: (1) the deep SS basins harboring the overwintering stock, (2) the Nova Scotia Current driven by outflow from the GSL, and (3) *C. finmarchicus* migrating to the surface layer in early spring in the Labrador Current that are transported in intrusion events of slope water onto the Shelf. *Head et al.* [1999] hypothesized that overwintering *C. finmarchicus* in the deep slope waters beyond the shelf break is a major source to the central and western SS. *C. finmarchicus* would be carried onto the SS from the slope region by intrusion of warm offshore water onto the mid-shelf in later winter-early spring. They put forward as a question whether the offshore source originates from an over-wintering stock in a local gyre-like system south of the SS or from advection in the

Labrador Current. They also asked whether *C. finmarchicus* advected off the SS are simply transported away from the region, or does a portion return to the slope to be retained in the proposed gyre. The model results here provide insights into these hypotheses and questions. The simulation shows important exchanges at the southern boundaries of both the LC and SS. The LC exported naupliar and early copepodids in May, when there was mainly import on the southern SS boundary (Figures 9i–9j). This may be a mechanism for transport from the LC to the SS via the shelf-break current that captures *C. finmarchicus* south of LC and transports them onto the SS. In contrast, deep-dwelling stages (CIV–V, CVd, and males) are imported from slope water into both the LC and the SS across the shelf break.

[48] The model results indicate that a large population develops in the slope water south of the SS. This area was initially devoid of animals, and was seeded by downward migration of the initial CVd population that had been carried to the southwestern boundary of the model domain (Figure 7). After the ascent of the freshly molted females, this stock was transported northward in the slope-water jet and then multiplied in warm (but not lethal) water. Little is known about the slope-water population of *C. finmarchicus*, but our simulated population is not unrealistic, as the presence of *C. finmarchicus* is known in the slope water south of New England [*Miller et al.*, 1991; *Ashjian et al.*, 2001]. *C. finmarchicus* has even been observed as far south as the mid-Atlantic Bight [*Judkins et al.*, 1979; *Smith and Lane*, 1988; *Lane et al.*, 1994], where it can develop vigorously following cold winters [*Grant*, 1988], and, for late copepodids and adults, as far east as the Gulf Stream at depth [*Wishner and Allison*, 1986; *Ashjian and Wishner*, 1993]. All these observations and analyses argue for a general southwestward transport of *C. finmarchicus* and a recirculation in the slope water, with the Gulf Stream as the ultimate southern boundary of its distribution in the North Atlantic.

[49] These results provide possible answers to the questions posed by *Head et al.* [1999] about the source of the shelf-break population and the subsequent fate of the on-shelf population. The hypothesis that emerges is that there are two sources of the shelf-break population: (1) exported LC individuals transported in the southwestward flow of the shelf-break current and (2) diapausing stage CV transported out of the SS in autumn/winter, a portion of which recirculates back onto the slope. The model predicts that these returning CV molt and reproduce in the slope water. The slope water south of Newfoundland and the SS is subject to marked interannual variability in dominance of either the warmer slope-water jet or the colder Labrador current [*Pickart et al.*, 1999], which would have a profound effect on the slope water *C. finmarchicus* stock [*Greene and Pershing*, 2000]. More observations are needed in the recirculation gyre south of the SS in order to determine the actual extent and frequency of reproduction in this area.

5. Concluding Remarks

[50] This study represents a first step in the evolution of a coupled physical-biological model that describes the dynamics of copepod populations in the GSL-SS system. Future refinements of the life-history model should be able to relate the diapause and spawning functions to seasonal variations of environmental variables, in particular phytoplankton abundance, for more accurate representations of seasonal and interannual variation in reproductive rates [e.g., *McLaren and Leonard*, 1995]. More explicit mortality functions, including the potential for increased cannibalism in low-chlorophyll waters [e.g., *Ohman and Hirche*, 2001], can be used to probe the relative influences of reproduction and mortality on population growth rates and interannual variation in *C. finmarchicus* life cycles. Future model runs will benefit as well from advances in physical modeling. As the life-cycle model allows multiyear simulations, a prognostic version of the physical model could link interannual variability in circulation and temperature with *C. finmarchicus* distribution and abundance. Refinements of the model will also require more observations in critical areas such as the southeast Labrador Sea, Newfoundland Shelf, and the Slope Water recirculation gyre, and observations of vertical distribution of *C. finmarchicus* particularly in strongly sheared areas like Cabot Strait and the shelf break.

[51] **Acknowledgments.** This work is a contribution to the GLOBEC-Canada program and was supported by grants from the Natural Sciences and Engineering Research Council and Fisheries and Oceans Canada. The technical contribution of P. Joly, M. Boulé, and P. Avendaño who assisted in the collection of data is gratefully acknowledged. We also thank M. Starr, who kindly provided the *C. finmarchicus* data set for Bonne Bay.

References

Aksnes, D. L., and J. Blindheim, Circulation patterns in the North Atlantic and possible impact on population dynamics of *Calanus finmarchicus*, *Ophelia*, *44*, 7–28, 1996.

Albikovskaya, L. K., and O. V. Gerasimova, Food and feeding patterns of cod (*Gadus morhua*, L.) and beaked redfish (S*ebastes mentella* Travin), *NAFO Sci. Counc. Stud.*, *19*, 31–39, 1993.

Anderson, J. T., Feeding ecology and condition of larval and pelagic juvenile redfish *Sebastes* spp., *Mar. Ecol. Prog. Ser.*, *104*, 211–226, 1994.

Ashjian, C. J., and K. F. Wishner, Temporal persistence of copepod species groups in the Gulf Stream, *Deep Sea Res.*, *40*, 483–516, 1993.

Ashjian, C. J., C. S. Davis, S. M. Gallager, and P. Alatalo, Distribution of plankton, particles, and hydrographic features across Georges Bank described using the Video Plankton Recorder, *Deep Sea Res., Part II*, *48*, 245–282, 2001.

Backhaus, J. O., I. H. Harms, M. Krause, and M. R. Heath, An hypothesis concerning the space-time succession of *Calanus finmarchicus* in the northern North Sea, *ICES J. Mar. Sci.*, *51*, 169–180, 1994.

Bamstedt, U., Life cycle, seasonal vertical distribution and feeding of *Calanus finmarchicus* in Skagerak coastal waters, *Mar. Biol.*, *137*, 279–289, 2000.

Bryant, A. D., D. Hainbucher, and M. Heath, Basin-scale advection and population persistence of *Calanus finmarchicus*, *Fish. Oceanogr.*, *7*, 235–244, 1998.

Campbell, R. G., J. A. Runge, and E. G. Durbin, Evidence of food limitation of *Calanus finmarchicus* production rates on the southern flank of Georges Bank during April 1997, *Deep Sea Res., Part II*, *48*, 531–549, 2001a.

Campbell, R. G., M. M. Wagner, G. J. Teegarden, C. A. Boudreau, and E. G. Durbin, Growth and development rates of the copepod *Calanus finmarchicus* reared in the laboratory, *Mar. Ecol. Prog. Ser.*, *221*, 161–183, 2001b.

Campbell, R. W., and E. J. H. Head, Viability of *Calanus finmarchicus eggs in situ*: Does the presence of intact phytoplankton reduce hatching success?, *ICES J. Mar. Sci.*, *57*, 1780–1785, 2000a.

Campbell, R. W., and E. J. H. Head, Egg production rates of *Calanus finmarchicus* in the western North Atlantic: Effect of gonad maturity, female size, chlorophyll concentration and temperature, *Can. J. Fish. Aquat. Sci.*, *57*, 518–529, 2000b.

Carlotti, F., and G. Radach, Seasonal dynamics of phytoplankton and *Calanus finmarchicus* in the North Sea as revealed by a coupled one dimensional model, *Limnol. Oceanogr.*, *41*, 522–539, 1996.

Colebrook, J. M., Continuous plankton records: Seasonal variations in the distribution and abundance of plankton in the North Atlantic and the North Sea, *J. Plankton Res.*, *4*, 435–462, 1982.

Cushing, D. H., The gadoid outburst in the North Sea, *J. Cons. Cons. Int. Explor. Mer.*, *41*(2), 159–166, 1984.

de Lafontaine, Y., S. Demers, and J. A. Runge, Pelagic food-web interactions and productivity in the gulf of St. Lawrence: A perspective, in *The gulf of St. Lawrence: Small ocean or big estuary*?, edited by J.-C. Therriault, *Can. Spec. Publ. Fish. Aquat. Sci.*, *113*, 99–123, 1991.

Diel, S., and K. Tande, Does the spawning of *Calanus finmarchicus* in high latitude follow a reproducible pattern, *Mar. Biol.*, *113*, 21–31, 1992.

Durbin, E. G., J. A. Runge, R. G. Campbell, P. R. Garrahan, M. C. Casas, and S. Plourde, Late fall-early winter recruitment of *Calanus finmarchicus* on Georges Bank, *Mar. Ecol. Prog. Ser.*, *151*, 103–114, 1997.

Durbin, E. G., P. R. Garrahan, and M. C. Casas, Abundance and distribution of *Calanus finmarchicus* on the Georges Bank during 1995 and 1996, *ICES J. Mar. Sci.*, *57*, 1664–1685, 2000a.

Durbin, E. G., P. R. Garrahan, and M. C. Casas, Depth distribution of *Calanus finmarchicus* naupliar on the Georges Bank during 1995 and 1996, *ICES J. Mar. Sci.*, *57*, 1686–1693, 2000b.

Edwards, A. M., and A. Yool, The role of higher predation in plankton population models, *J. Plankton Res.*, *22*, 1085–1112, 2000.

El-Sabh, M. I., The lower St. Lawrence estuary as a physical oceanographic system, *Nat. Can.*, *106*, 55–73, 1979.

Filteau, G., and J.-L. Tremblay, Ecologie de *Calanus finmarchicus* dans la Baie des Chaleurs, *Nat. Can.*, *80*, 5–79, 1953.

Fossum, P., and B. Ellertsen, Gut content analysis of first-feeding cod larvae (*Gadus morhua* L.) sampled at Lofoten, Norway, in *Cod and Climate Change: Proceedings of a Symposium Held in Reykjavik, 23–27 August 1993*, edited by J. Jakobsson et al., *ICES Mar. Sci. Symp.*, *198*, 430–437, 1994.

Gaard, E., The zooplankton community structure in relation to its biological and physical environment on the Faroe shelf, 1989–1997, *J. Plankton Res.*, *21*, 1133–1152, 1999.

Gaard, E., Seasonal abundance and development of *Calanus finmarchicus* in relation to phytoplankton and hydrography on the Faroe shelf, *ICES J. Mar. Sci.*, *57*, 1605–1611, 2000.

Gislasson, A., and O. S. Astthorsson, Seasonal development of *Calanus finmarchicus* along an inshore-offshore gradient southwest of Iceland, *Ophelia*, *44*, 71–84, 1996.

Gislasson, A., O. S. Astthorsson, H. Petursdottir, H. Gudfinnsson, and A. R. Bodvarsdottir, Life cycle of *Calanus finmarchicus* south of Iceland in relation to hydrography and chlorophyll *a*, *ICES J. Mar. Sci.*, *57*, 1619–1627, 2000.

Grant, G. C., Seasonal occurrence and dominance of *Centropages* congeners in the Middle Atlantic Bight, USA, in *Biology of Copepods*, edited by G. A. Boxshall and H. K. Schminke, *Hydrobiologia*, *167/168*, 223–227, 1988.

Greene, C. H., and A. J. Pershing, The response of *Calanus finmarchicus* populations to climate variability in the Northwest Atlantic: Basin-scale forcing associated with the North Atlantic Oscillation, *ICES J. Mar. Sci.*, *57*, 1536–1544, 2000.

Grigg, H., and S. J. Bardwell, Seasonal observations on moulting and maturation in stage V copepodites of *Calanus finmarchicus* from the Firth of Clyde, *J. Mar. Biol. Assoc. U. K.*, *62*(2), 315–327, 1982.

Hannah, C. G., C. E. Naimie, J. W. Loder, and F. E. Werner, Upper-ocean transport mechanisms from the Gulf of Maine to Georges Bank, with implications for *Calanus* supply, *Cont. Shelf Res.*, *15*, 1887–1912, 1998.

Hansen, B., E. Gaard, and J. Reinert, Physical effects on recruitment of Faroe Plateau cod, in *Cod and Climate Change*: *Proceedings of a Symposium Held in Reykjavik, 23–27 August 1993*, edited by J. Jakobsson et al., *ICES Mar. Sci. Symp.*, *198*, 520–528, 1994.

Head, E. J. H., L. R. Harris, and B. Petrie, Distribution of *Calanus* spp. on and around the Nova Scotia shelf in April-Evidence for an offshore source of Calanus finmarchicus to the mid- and western regions, *Can. J. Fish. Aquat. Sci.*, *56*, 2463–2476, 1999.

Head, E. J. H., L. R. Harris, and R. W. Campbell, Investigations on the ecology of Calanus spp. In the Labrador Sea: I. Relationship between the phytoplankton bloom and reproduction and development of *Calanus finmarchicus* in spring, *Mar. Ecol. Prog. Ser.*, *193*, 53–73, 2000.

Heath, M. R., J. G. Fraser, A. Gislason, S. J. Hay, S. H. Jonasdottir, and K. Richardson, Winter distribution of *Calanus finmarchicus* in the northeast Atlantic, *ICES J. Mar. Sci.*, *57*, 1628–1635, 2000.

Herman, A. W., D. D. Sameoto, S. Chen, M. R. Mitchell, B. Petrie, and N. Cochrane, Sources of zooplankton on the Nova Scotia and their aggregations within deep-shelf basins, *Cont. Shelf Res.*, *11*, 211–238, 1991.

Hind, A., W. S. C. Gurney, M. Heath, and A. D. Bryant, Overwintering strategies in *Calanus finmarchicus*, *Mar. Ecol. Prog. Ser.*, *193*, 95–107, 2000.

Hirche, H. J., The reproductive biology of the marine copepod, *Calanus finmarchicus*–A review, *Ophelia*, *44*, 111–128, 1996a.

Hirche, H. J., Diapause in the marine copepod, *Calanus finmarchicus*–A review, *Ophelia*, *44*, 129–143, 1996b.

Ingram, R. G., and M. I. El-Sabh, Fronts and mesoscale features in the St. Lawrence estuary, in *Oceanography of a Large-Scale Estuarine System: The St. Lawrence*, edited by M. I. El-Sabh and N. Silverberg, *Coastal Estuarine Stud.*, *39*, 71–93, 1990.

Irigoien, X., Vertical distribution and population structure of *Calanus finmarchicus* at Station India (59 degrees N, 9 degrees W) during the passage of the great salinity anomaly, *Deep Sea Res., Part I*, *47*, 1–26, 2000.

Judkins, D. C., C. D. Wirick, and W. E. Esaias, Composition, abundance, and distribution of zooplankton in the New York Bight, September 1974–September 1975, *Fish. Bull.*, *77*, 669–683, 1979.

Koutitonsky, V. G., Transport de masses d'eau à l'embouchure de l'estuaire du Saint-Laurent, *Nat. Can.*, *106*, 75–88, 1979.

Koutitonsky, V. G., and G. L. Bugden, The physical oceanography of the Gulf of St. Lawrence: A review with emphasis on the synoptic variability of the motion, in *The Gulf of St. Lawrence: Small Ocean or Big Estuary?*, edited by J.-C. Therriault, *Can. Spec. Publ. Fish. Aquat. Sci*., *113*, 57–90, 1991.

Lane, P. V. Z., S. L. Smith, J. L. Urban, and J. L. Biscaye, Carbon flux and recycling associated with zooplankton fecal pellets on the shelf of the Middle Atlantic Bight, *Deep Sea Res., Part II*, *41*, 437–457, 1994.

Lu, Y., K. R. Thompson, and D. G. Wright, Tidal currents and mixing in the Gulf of St. Lawrence: An application of the incremental approach to data assimilation, *Can. J. Fish. Aquat. Sci.*, *58*, 723–735, 2001.

Lynch, D. R., W. C. Gentleman, D. J. McGillicuddy Jr., and C. S. Davis, Biological/physical simulations of *Calanus finmarchicus* population dynamics in the Gulf of Maine, *Mar. Ecol. Prog. Ser.*, *169*, 189–210, 1998.

Mackas, D. L., and B. de Young, GLOBEC Canada 1996–2000: A sampler, *Can. J. Fish. Aquat. Sci.*, *58*, 645–646, 2001.

Marshall, S. M., and A. P. Orr, *The Biology of A Marine Copepod*, Oliver and Boyd, Edinburgh, 1955.

McLaren, I. A., and A. Leonard, Assessing the equivalence of growth and egg production of copepods, *ICES J. Mar. Sci.*, *52*, 397–408, 1995.

McLaren, I. A., J.-M. Sevigny, and C. J. Corkett, Body sizes, development rates and genome sizes among *Calanus* species, *Hydrobiologia*, *167/168*, 275–284, 1988.

McLaren, I. A., E. Head, and D. D. Sameoto, Life cycles and seasonal distributions of *Calanus finmarchicus* on the central Scotian Shelf, *Can. J. Fish. Aquat. Sci.*, *58*, 659–670, 2001.

Meise, C. J., and J. E. O'Reilly, Spatial and seasonal patterns in abundance and age-composition of *Calanus finmarchicus* in the Gulf of Maine and on Georges Bank: 1977–1987, *Deep Sea Res., Part II*, *43*, 1473–1501, 1996.

Miller, C. B., and K. S. Tande, Stage duration estimations for *Calanus* populations: A modelling study, *Mar. Ecol. Prog. Stud.*, *102*(1–2), 15–34, 1993.

Miller, C. B., T. J. Cowles, P. H. Wiebe, N. J. Copley, and H. Grigg, Phenology in *Calanus finmarchicus*: Hypotheses about control mechanisms, *Mar. Ecol. Prog. Ser.*, *72*, 79–91, 1991.

Miller, C. B., D. R. Lynch, F. Carlotti, W. Gentlemen, and C. V. W. Lewis, Coupling of an individual-based population dynamic model of *Calanus finmarchicus* to a circulation model for the Georges Bank region, *Fish. Oceanogr.*, *7*, 219–234, 1998.

Ohman, M. D., and H. J. Hirche, Density-dependent mortality in an oceanic copepod population, *Nature*, *412*(6847), 638–641, 2001.

Ohman, M. D., and J. A. Runge, Sustained fecundity when phytoplankton resources are in short supply: Omnivory by *Calanus finmarchicus* in the Gulf of St. Lawrence, *Limnol. Oceanogr.*, *39*, 21–36, 1994.

Ohman, M. D., J. A. Runge, E. G. Durbin, D. B. Field, and B. Niehoff, On birth and death in the sea, *Hydrobiologia*, *480*, 55–68, 2003.

Orlanski, I., A simple boundary condition for unbounded hyperbolic flows, *J. Comput. Phys.*, *21*, 251–269, 1976.

Paffenhöfer, G.-A., J. R. Strickler, K. D. Lewis, and S. Richman, Motion behavior of nauplii and early copepodid stages of marine planktonic copepods, *J. Plankton Res.*, *18*, 1699–1715, 1996.

Pedersen, O. P., K. S. Tande, and D. Slagstad, A model study of demography and spatial distribution of *Calanus finmarchicus* at the Norwegian coast, *Deep Sea Res., Part II*, *48*, 567–587, 2001.

Petrie, B., K. Drinkwater, A. Sanström, R. Petipas, D. Gregory, D. Gilbert, and P. Sekhon, Temperature, salinity and sigma-t atlas for the Gulf of St. Lawrence, *Can. Tech. Rep. Hydrogr. Ocean Sci.*, *178*, v + 256 pp., 1996.

Pickart, R. S., T. K. McKee, D. J. Torres, and S. A. Harrington, Mean structure and inter-annual variability of the slope water system south of Newfoundland, *J. Phys. Oceanogr.*, *29*, 2541–2558, 1999.

Planque, B., and S. D. Batten, *Calanus finmarchicus* in the North Atlantic: The year of *Calanus* in the context of inter-decadal changes, *ICES J. Mar. Sci.*, *57*, 1528–1535, 2000.

Planque, B., G. C. Hays, F. Ibanez, and J. C. Gamble, Large scale variations in the seasonal abundance of *Calanus finmarchicus*, *Deep Sea Res., Part I*, *44*, 315–326, 1997.

Plourde, S., and J. A. Runge, Reproduction of the planktonic copepod *Calanus finmarchicus* in the lower St. Lawrence Estuary: Relation to the cycle of phytoplankton production and evidence for a *Calanus* pump, *Mar. Ecol. Prog. Ser.*, *102*, 217–227, 1993.

Plourde, S., P. Joly, J. A. Runge, B. Zakardjian, and J. J. Dodson, Life cycle of *Calanus finmarchicus* in the lower St. Lawrence Estuary: The imprint of circulation and late timing of the spring phytoplankton bloom, *Can. J. Fish. Aquat. Sci.*, *58*, 647–658, 2001.

Roache, P. J., *Computational Fluid Dynamics*, revised ed., Hermosa, Albuquerque, N. M., 1976.

Runge, J. A., Should we expect a relationship between primary production and fisheries? The role of copepod dynamics as a filter of trophic variability, *Hydrobiologia*, *167/168*, 61–71, 1988.

Runge, J. A., and Y. de Lafontaine, Characterization of the pelagic ecosystem in surface waters of the northern Gulf of St. Lawrence in early summer: The larval redfish-*Calanus*-microzooplankton interaction, *Fish. Oceanogr.*, *5*, 21–37, 1996.

Runge, J. A., and S. Plourde, Fecundity characteristics of *Calanus finmarchicus* in coastal waters of eastern Canada, *Ophelia*, *44*, 171–187, 1996.

Runge, J. A., and Y. Simard, Zooplankton in the St. Lawrence Estuary: The imprint of physical processes on its composition and distribution, in *Oceanography of a Large-Scale Estuarine System: The St. Lawrence*, edited by M. I. El-Sabh and N. Silverberg, *Coastal Estuarine Stud.*, *39*, 296–320, 1990.

Runge, J. A., M. Castonguay, Y. de Lafontaine, M. Ringuette, and J.-L. Beaulieu, Covariation in climate, zooplankton biomass and mackerel recruitment in the southern Gulf of St. Lawrence, *Fish. Oceanogr.*, *8*, 139–149, 1999.

Sameoto, D. D., and A. W. Herman, Effect of the outflow from the Gulf of St. Lawrence on Nova Scotia shelf zooplankton, *Can. J. Fish. Aquat. Sci.*, *49*, 857–869, 1992.

Sameoto, D. D., J. Neilson, and D. Waldron, Zooplankton prey selection by juvenile fish in Nova Scotian shelf basins, *J. Plankton Res.*, *16*, 1003–1019, 1994.

Sheng, J. Y., Dynamics of a buoyancy-driven coastal jet: The Gaspe Current, *J. Phys. Oceanogr.*, *31*, 3146–3162, 2001.

Sheng, J., and L. Tang, A numerical study of circulation in the western Caribbean Sea, *J. Phys. Oceanogr.*, *33*, 2049–2069, 2003.

Sheng, J., D. G. Wright, R. J. Greatbatch, and D. E. Dietrich, CANDIE: A new version of the DieCAST ocean circulation model, *J. Atmos. Oceanic Technol.*, *15*, 1414–1432, 1998.

Sheng, J., R. J. Greatbatch, and D. Wright, Improving the utility of ocean circulation models through adjustment of the momentum balance, *J. Geophys. Res.*, *106*(C8), 16,711–16,728, 2001.

Sheng, J., K. R. Thompson, M. Dowd, and B. Petrie, Seasonal mean circulation over the eastern Canadian shelf, with emphasis on the Gulf of St. Lawrence and Scotian Shelf, *J. Geophys. Res.*, (in revision), 2003.

Shore, J. A., C. G. Hannah, and J. W. Loder, Drift pathways on the western Scotian Shelf and its environs, *Can. J. Fish. Aquat. Sci.*, *57*, 2488–2505, 2000.

Skreslet, S., A conceptual model of the trophodynamical response to river discharge in a large marine ecosystem, *J. Mar. Syst.*, *12*, 187–198, 1997.

Slagstad, D., and K. S. Tande, The importance of seasonal vertical migration in across shelf transport of *Calanus finmarchicus*, *Ophelia*, *44*, 189–205, 1996.

Smith, S. L., and P. V. Z. Lane, Grazing of the spring diatom bloom in the New York Bight by the calanoid copepods *Calanus finmarchicus*, *Metridia lucens* and *Centropages typicus*, *Cont. Shelf. Res.*, *8*, 485–509, 1988.

Starr, M., J.-C. Therriault, G. Y. Conan, M. Comeau, and G. Robichaud, Larval release in a sub-euphotic zone invertebrate triggered by sinking phytoplankton particles, *J. Plankton Res.*, *16*, 1137–1147, 1994.

Sundby, S., Recruitment of Atlantic cod stocks in relation to temperature and advection of copepod populations, *Sarsia*, *85*, 277–298, 2001.

Tande, K. S., Ecological investigations on the zooplankton community of Balsfjorden, Northern Norway: Generation cycles, and variations in body weight and body content of carbon and nitrogen related to overwintering and reproduction in the copepod *Calanus finmarchicus* (Gunnerus), *J. Exp. Mar. Biol. Ecol.*, *62*, 129–142, 1982.

Tande, K. S., An evaluation of factors affecting vertical distribution among recruits of *Calanus finmarchicus* in three adjacent high-latitude localities, *Hydrobiologia*, *167/168*, 115–126, 1988.

Tande, K. S., and C. B. Miller, Population dynamics of *Calanus* in the North Atlantic: Results from the trans-Atlantic study of *Calanus finmarchicus*, *ICES J. Mar. Sci.*, *57*, 1527, 2000.

Tande, K. S., and D. Slagstad, Regional and inter-annual variations in biomass and productivity of the marine copepods, *Calanus finmarchicus*, in sub-arctic environment, *Oceanol. Acta*, *15*, 309–321, 1992.

Therriault, J.-C., et al., Proposal for a northwest Atlantic zonal monitoring program, *Can. Tech. Rep. Hydrogr. Ocean Sci.*, *194*, vii + 57 pp., 1998.

Tremblay, M. J., and J. C. Roff, Community gradients in the Scotian Shelf zooplankton, *Can. J. Fish. Aquat. Sci.*, *40*, 598–611, 1983.

Vidal, J., Physioecology of zooplankton: I. Effects of phytoplankton concentration, temperature and body size on the growth rate of *Calanus pacificus* and *Pseudocalanus* sp., *Mar. Biol.*, *56*, 111–134, 1980.

Wiebe, P. H., R. C. Beardsley, D. G. Mountain, and A. Bucklin, Global Ocean Ecosystem Dynamics-Initial program in northwest Atlantic, *Sea Technol.*, *37*(8), 67–76, 1996.

Wishner, K. F., and S. K. Allison, The distribution and abundance of copepods in relation to the physical structure of the Gulf Stream, *Deep Sea Res., Part A*, *33*, 705–731, 1986.

Wroblewski, J. S., Interaction of currents and vertical migration in maintaining *Calanus marshallae* in the Oregon upwelling zone-A simulation, *Deep Sea Res., Part A*, *29*, 665–686, 1982.

Yamazaki, H., and K. D. Squires, Comparison of oceanic turbulence and copepod swimming, *Mar. Ecol. Prog. Ser.*, *144*, 299–301, 1996.

Zakardjian, B. A., J. A. Runge, S. Plourde, and Y. Gratton, A biophysical model of the interaction between vertical migration of crustacean zooplankton and circulation in the lower St. Lawrence Estuary, *Can. J. Fish. Aquat. Sci.*, *56*, 2420–2432, 1999.

Zakardjian, B. A., Y. Gratton, and A. F. Vézina, Late spring phytoplankton bloom in the lower St. Lawrence Estuary: The flushing hypothesis revisited, *Mar. Ecol. Prog. Ser.*, *192*, 31–48, 2000.

Y. Gratton, INRS-Eau, 2800 rue Einstein, C.P. 7500, Sainte-Foy, Quebec, G1V 4C7, Canada. (yves_gratton@inrs-ete.uquebec.ca)

I. McLaren, Department of Biology, Dalhousie University, Halifax, N. S., B3H 4J1, Canada. (iamclare@is.dal.ca)

S. Plourde, Fisheries and Ocean Canada, Maurice Lamontagne Institute, 850 Route de la Mer, Mont-Joli, Quebec G5H 3Z4, Canada. (plourdes@dfo-mpo.gc.ca)

J. A. Runge, Ocean Process Analysis Laboratory, University of New Hampshire, 142 Morse Hall, Durham, NH 03824, USA. (jrunge@cisunix.unh.edu)

J. Sheng and K. R. Thompson, Department of Oceanography, Dalhousie University, Halifax, N. S., B3H 4J1 Canada. (sheng@phys.ocean.dal.ca; keith@phys.ocean.dal.ca)

B. A. Zakardjian, Institut des Sciences de la Mer de Rimouski (ISMER), Université du Québec à Rimouski, 310 Allée des Ursulines, Rimouski, Que., G5L 3A1, Canada. (bruno_zakardjian@uqar.uquebec.ca)